# Investigation of structural, dielectric, ferroelectric and optical properties of $SrTiO_3$ doped $(K,Na)NbO_3$ ceramics

*A thesis submitted in partial fulfilment of the requirements for the award of*

*Degree of*

**Master of Science**

**In**

**Physics**

**Submitted by**

**Prinka Rani**

**Reg. No. 301704022**

**Under the supervision of**

**Dr. Poonam Uniyal**

**Associate Professor**


**School of Physics and Materials Science**

**Thapar Institute of Engineering and Technology,**

**Patiala (punjab)-147001, INDIA**

**July 2019**

## CERTIFICATE

I, hereby declare that the work which has been presented in this thesis entitled **"Investigation of structural,dielectric,ferroelectric and optical properties of $SrTiO_3$ doped $(K,Na)NbO_3$ ceramics"** is an authentic record of my own work carried out for the partial fulfilment of the requirement for the award of the degree of Masters of Science in Physics at ThaparInstitute Of Engineering And Technology, Patiala (Punjab), under the guidance of **Dr. Poonam Uniyal,** Associate Professor, School of Physics and Materials Science. The intellectual content of this thesis is the product of my own work and contains no material which to a substantial extent has been accepted for the award of any other degree at this or any other educational institution, except where due acknowledgment is made in the thesis.

Prinka Rani

(Prinka Rani)
Roll no.: 301704022

Poonam

**Dr. Poonam Uniyal**

**Associate Professor**

**SPMS,**

**Thapar Institute of Engineering and Technology, Patiala**

# ACKNOWLEDGEMENT

Work on this thesis would not have been possible without the encouragement and the support of many people. I would like to express my sincere gratitude especially to the following:

The first and greatest thank to my supervisor **Dr. Poonam Uniyal, Associate Professor, School of Physics and Material Science, Thapar Institute of Engineering and Technology, Patiala,** for his continuous support and supervision, for his excellent guidance, patience, motivation and enthusiasm.

I would like to thank **Dr. O.P Pandey**, Professor and Head, SPMS for providing me with an excellent atmosphere and all the necessary facilities for my research. Besides, my supervisor, I would like to thank from the bottom of my heart, **Mrs. Kamaldeep Kaur** for sharing their valuable experiences. I would not have been able to complete my dissertation without their cooperation.

I would like to acknowledge my lab mate Anjali Mehta who supported me at each step.

I would like to thank my friends Gurpreet Singh, Shivangi Bhatia, and Baneet Chawla being their always with me.

Last but not the least; I would like to thank my parents and my brother for their unconditional support, both financially and emotionally throughout my degree.

Above all I render my gratitude to the almighty who bestowed upon me the strength and vision to walk on the path of truth.

***I dedicate this work to my loving parents, my brother and my friends who encouraged and supported me.***

# ABSTRACT

All lead-based ceramics show excellent electromechanical properties but due to toxicity of lead researchers have focused their attention on lead free ceramics such as $(BiNa)TiO_3$, $(K,Na)NbO_3$ etc. $(K,Na)NbO_3$ ceramics find applications for sensors, actuators, transducers and high energy storage.

Samples of $(1-x)(K,Na)NbO_3$-$(x)SrTiO_3$ ceramics for composition x=0, 0.1, 0.2 were synthesized using solid-state route and samples were studied for structural, dielectric, ferroelectric and optical properties. Single phase $(K,Na)NbO_3$ ceramics were obtained. On addition of $SrTiO_3$ a coexistence of orthorhombic-tetragonal symmetry is observed. A decrease in grain size is also observed. The dielectric properties were studied in wide temperature range of $50^oC$ to $500^oC$ at frequency varying from 100Hz to 1MHz. Room temperature ferroelectric hysteresis loops were measured for all the synthesized compositions. Dependence of remnant polarization and coercive field on $SrTiO_3$ concentration indicates decrease in energy loss and increase in energy storage density.

## *Table of Contents*



## *Chapter1: Introduction*

## *Chapter2: Literature Survey*



## *Chapter3: Synthesis and Characterization Techniques*

## *List of Figures*

## *List Of Tables*

**ε'** dielectric constant

**tanδ** dielectric loss

$\mathbf{P_r}$ remanent polarization

$\mathbf{E_c}$ coercive field

$\mathbf{P_{max}}$ maximum polarization

$\mathbf{E_{max}}$ maximum electric field

**a, b, c** lattice parameters

$\mathbf{T_C}$ Curie temperature

$\mathbf{d_{33}}$ piezoelectric coefficient

$\mathbf{K_p}$ electromechanical coupling constant

$\mathbf{K_t}$ thickness coupling coefficient

**Z'** real impedance

**Z''** imaginary impedance

$W_{rec}$ recoverable energy storage density

**θ** diffraction angle

**KNN** Potassium Sodium Niobate

**BNT** Bismuth Sodium Titanate

**PT** Lead Titanate

**PZT** Lead Zirconate Titanate

**ST** strontium Titanate

**LN** Lithium Niobate

**LT** Lithium Tantalate

**KN** Potassium Niobate

**NN** Sodium Niobate

# *Chapter:1*
# *Introduction*

## 1.1. Introduction

Nowadays, electric power is assumed as a backbone of modern society and electronic industry. The energy storage is an effective method for efficient use of energy as this method reduces the depletion of fossil fuels and global warming[1].The most commonly used energy storage devices are sodium/lithium batteries, electrochemical capacitors, fuel cells, and electrostatic capacitors. But lead-based, lead-free ferroelectrics and dielectric ceramics with perovskite structure are more effective sources of energy storage due to their high polarization and external electric field[2].

In recent past years, lead-based ferroelectric ceramics with perovskite structure such as Lead titanate(PT) and Lead zirconate titanate(PZT) are used for electronic applications such as sensors, transformers and for piezoelectric transducers etc. due to its outstanding electrical and mechanical properties. But lead is highly poisonous and harmful material. Lead can cause damage to human neural structure, kidneys and nervous system and also has some impact on environment and climate change. It is really difficult to get rid of lead content from the human body[3]. As an alternative, in recent years, many lead-free perovskite materials such as sodium bismuth titanate (NBT), barium titanate (BT), potassium tantalate niobate (KTN) and sodium potassium niobate (NKN) have seeked a lot of attention from researchers. These all are the promising lead-free ferroelectric systems with perovskite structure. These all exhibit very good ferroelectric, piezoelectric and pyroelectric properties especially close to morphotropic phase boundary (MPB) similarly as lead-contained materials[4-5].

Out of these non lead contained ferroelectric materials potassium sodium niobate (KNN) is assumed as a good candidate due to its excellent electromechanical properties. (K, Na)$NbO_3$ is a solid solution with composition of K/Na near 50/50 at morphotropic phase boundary. The KNN ceramics exhibits orthorhombic crystalline symmetry at room temperature with space group $mm_2$ and through this space group KNN ceramics establish possible number of domain wall orientations[5] . KNN solid solutions can be synthesized by various techniques such as chemical vapour deposition, sol-gel, solid-state reaction, and hydro-thermal.

## 1.2. Perovskite Structure

As well known, most of lead-contained and non lead-contained ceramics are unique class of perovskite-structured ceramics which exhibit good electromechanical properties. Perovskite material is a mineral with $ABX_3$ structure in which ions located at 'A-site and B-site' are cations and ions located at 'X-site' are anions, which was firstly found to Gustav Rose from the Ural Mountains of Russia in 1839. But its name based on Russian mineralogist L. A. Perovski. Perovskite unit cell corresponds to $A^{a+}$ (8), $B^{b+}$(1), and $O^{2-}$(6) ions shown in fig.1.1. In perovskite unit cell larger $A^{a+}$ ($K^{+1}$, $Na^{+1}$, $Bi^{+2}$, $Ca^{+2}$, $Li^{+1}$, and $Sr^{+2}$) ions presented at corners of unit cell, small ion $B^{b+}$ ($Nb^{+5}$, $Ti^{+4}$, and $Ta^{+5}$)presented at the octahedral site of a unit cell and six $O^{2-}$ ions are at faces of a unit cell. Larger $A^{a+}$ cations are attached by 12 $O^{2-}$ anion and $B^{b+}$ cations are attached by 6 $O^{2-}$anions. In these materials, 1/2 of each oxygen atom and 1/8 of each A-site ion belong to the cubic structure. And due to excellent electromechanical properties, crystalline materials with perovskite structure are widely used for industrial applications. Some complex perovskite structure based ceramics contain two different types of A-site cations for example (K, Na) $NbO_3$, (Bi, Na) $TiO_3$, $CaTiO_3$, $SrTiO_3$, and $LiTaO_3$ceramics. In these perovskite examples, $K^{+1}$, $Na^{+1}$, $Bi^{+2}$, $Ca^{+2}$, $Li^{+1}$, and $Sr^{+2}$ ions are placed on A-site of crystal structure and $Nb^{+5}$, $Ti^{+4}$, and $Ta^{+5}$ ions placed on B-site of crystal structure.

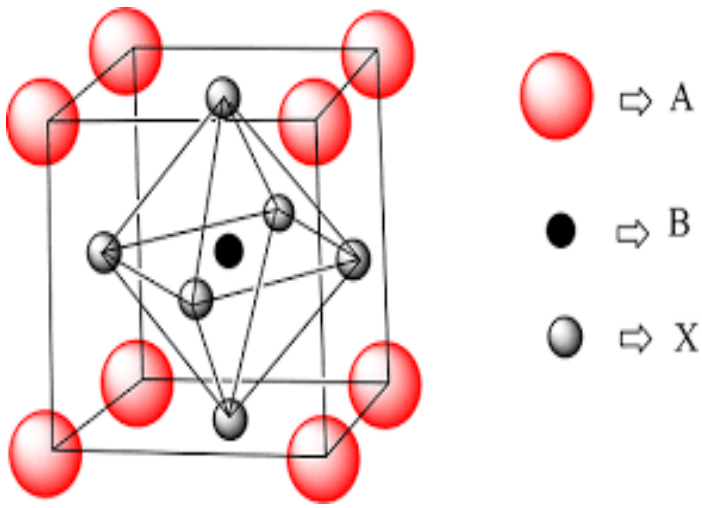


**FIGURE 1.1: Schematic diagram of Perovskite structure**

## 1.3. Ferroelectrics

Ferroelectric materials are materials that exhibit the property of spontaneous polarization (P) even after electric field (E) is turned off. Ferroelectrics are based on ferroelectricity pheonomenon which was discovered by Valasek in1920 and this phenomenon was first observed in Rochelle salt in 1921. Ferroelectricity is defined as a property in which intrinsic polarization of material turned into reverse direction as a function of external applied electric field (E). In ferroelectrics, arrangement of anions and cations obtained the electric dipole moments within unit cells of crystal and because of this, materials polarization can be observed by its surface current. Ferroelectric materials do not possess center of symmetry. Out of 32 possible crystal classes, eleven crystal classes exhibit centro-symmetry and hence these crystal classes cannot exhibit ferroelectricity. Ferroelectric ceramics can show good piezoelectric and pyroelectric behaviour, but reverse is not true.[6]

### 1.3.1 Types of Ferroelectrics

On behalf of relative permitivity vs. Frequency curve and relative permittivity vs. Temperature curve, ferroelectrics has two types:

**Normal ferroelectrics:** In these type of ferroelectrics, sharp phase transitions from ferroelectric to paraelectric state at critical or curie temperature is seen in the dielectric study. A most common example of "normal" ferroelectric material is Barium titanate(BT) in which ferroelectric phase transition occurs at 120˚C temperature[7]. Normal ferroelectrics exhibit strong remanent polarization. In normal ferroelectrics, line splitting of x-rays occurs [8]. Normal ferroelectric materials follow Curie-Weiss law but exhibit low frequency response. About $T_C$, normal ferroelectrics do not display any hysteresis curve.

**Relaxor ferroelectrics:** Relaxor ferroelectric materials show more gradual variation of permittivity or dielectric peaks that exhibit broad-diffuse phase transitions. often "relaxor" ferroelectrics carry more than 2 cations. Commonly studied lead-based relaxors are lead zirconate titanate(PZT), lead magnesium niobate(PMN) or lead-free relaxors are sodium bismuth titanate(NBT), potassium sodium niobate (KNN). In "relaxor" ferroelectrics, broad peaks of permittivity do not always indicate a structural phase transformations, therefore temperature value of the maximum permittivity peak is specified by $T_M$ instead of $T_C$. They show high frequency values, low ferroelectric properties such as remanent polarization, corecive field and low anisotropy. About $T_C$, relaxors exhibit hysteresis loop[7-8].

## 1.4. Characteristics of Ferroelectrics

### 1.4.1. Structural symmetry

Structural symmetry of ferroelectric materials can be identified by lattice parameters of crystal. Thousands of crystals exist in nature but all correspond to 32 macroscopic symmetry types or 32 point groups shown in table1.1. From these 32 symmetry types, some are centro symmetries and some are non centro symmetries. Out of 32, ten point groups are showing centro-symmetry property and 21 point groups show non centro- symmetries. Only non-center symmetry point group exhibit ferroelectricity**.**

**Table 1.1. 32 Point groups of crystal structures**

| Crystal Class | Bravais Lattices | Point Groups |
|---|---|---|
| Triclinic | P | 1, $\bar{1}$ |
| Monoclinic | P, C | 2, m, 2/m |
| Orthorhombic | P, C, F, I | 222, mm2, 2/m 2/m 2/m |
| Trigonal | P, R | 3, $\bar{3}$, 32, 3m, $\bar{3}$2/m |
| Hexagonal | P | 6, $\bar{6}$, 6/m, 622, 6mm, $\bar{6}$m2, 6/m 2/m 2/m |
| Tetragonal | P, I | 4, $\bar{4}$, 4/m, 422, 4mm, $\bar{4}$2m, 4/m 2/m 2/m |
| Isometric | P, F, I | 23, 2/m$\bar{3}$, 432, $\bar{4}$3m, 4/m$\bar{3}$2/m |

Crystal symmetry of ferroelectrics affects the physical and structural properties of ferroelectric material such as elastic, dielectric, ferroelectric, piezoelectric and optical properties[9].

### 1.4.2. Piezoelectric properties

Piezoelectric phenomenon co-authored by Pierre Curie and Jacques Curie in 1880 by conducting a variety of experiments on the range of crystals. In piezoelectric phenomenon, the electric charge generated in response to external mechanical stress. Ferroelectric materials exhibit large piezoelectric properties. Through polling process, lead-based ferroelectrics show high $d_{33}$(piezoelectric constant) value and lead-free materials also exhibits high $d_{33}$value. Out of 32 crystal point groups, 21 point groups do not have centro-symmetry and these all show ferroelectricity and out of these 21, twenty point groups exhibit piezoelectricity. All ferroelectric materials are inherently piezoelectric materials.[9]

### 1.4.3. Pyroelectric properties

Pyroelectricity was discovered by Teophrast in tourmaline named material and its name was coined by Brewster in 1824. Pyroelectricity is an electric phenomenon in which electric potential generates when materials are cooled or heated. The sign of pyroelectric coefficient 'p' is based on the orientation of the piezoelectric axis of ferroelectric material. All pyroelectric materials are piezoelectric.

### 1.4.4. Ferroelectric hysteresis loop

The ferroelectric hysteresis loop is a curve of polarization and electric field(P-E loop). In the P-E loop, polarization is a double-valued property which respond to applied electric field. With little amount of applied field value, linear relationship between E and P exhibited, because with little amount of field ferroelectric domains cannot switch and at this stage crystal only behave like dielectric material. This corresponds to the segment OA of ferroelectric curves shown in Figure 1.2. When electric field increases, then negative domains(which show polarization opposite to field) will be switched over in a positive way(which is direction of electric field) and polarization will increase(segmented) and this process ends at segment BC, because this segment is in saturation state and at this state ferroelectric crystal is composed of single domain.When the electric field decreases, then polarization also starts decreasing only by not returning to zero. When the electric field is decreased to zero, few domains will remain aligned in the positive route and ferroelectric crystal will show a remanent polarization($P_r$). The extrapolation of saturation segment BC back to the polarization axis at point E(shown in Figure.1.2) shows the value of spontaneous polarization ($P_s$). Remanent polarization $P_r$ can be removed only with reversed applied electric field which is shown at point F in given Figure.1.2. And this reversed applied electric field is referred as coercive field ($E_c$). The increase of applied electric field in a negative route will cause the alignment of dipoles and reversing the electric field once again can complete the cycle and this relationship of polarization and an electric field is known as the hysteresis loop which is shown in Figure 1.2 in form of 'CDFGHC'[10].

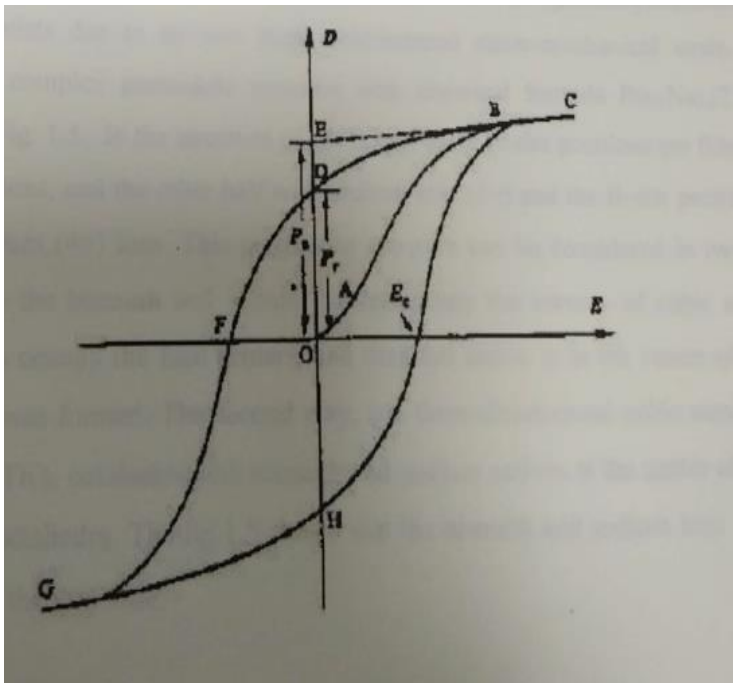


**Figure 1.2: Schematic diagram of a ferroelectric hysteresis loop [9].**

## 1.5 Potassium Sodium Niobate (KNN)

KNN is good non lead-contained ferroelectric material which exhibits excellent ferroelectric properties and that properties are compatible with lead-based materials and it was first established by Saito et al. for exchange lead-based ceramics [11]. KNN is a solution which is composed of sodium niobate(SN) and potassium niobate(KN) ceramics. In KNN solid solution, Na/K is 50/50 and this Na/K composition being near to morphotropic phase boundary(MPB)[12]. $(K,Na)NbO_3$ is a highly researched material. From some past years to reduce the use of lead-based materials, KNN solid solution was studied by many researchers.

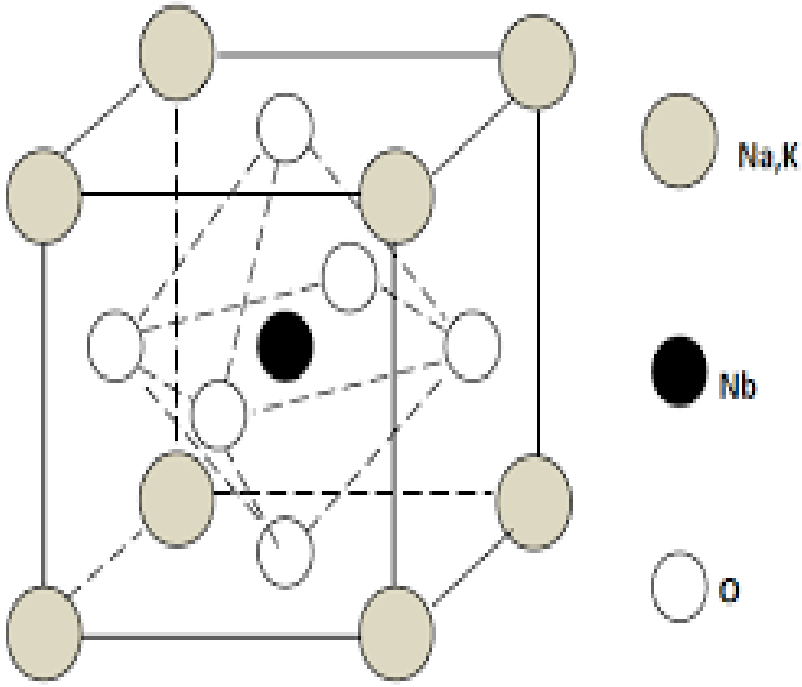


- **Figure 1.3: Schematic diagram of crystal structure of (K, Na)$NbO_3$ ceramics[13]**

### 1.5.1. Properties KNN material

Potassium Sodium Niobate materials depicts interesting properties such as high curie temperature $T_c$(~420˚C), good electromechanical coupling constant $k_{33}$(~0.36), high piezoelectric constant $d_{33}$(~80pC/N). KNN ceramics also depicts low dielectric properties at high frequencies such as dielectric constant ($\varepsilon_r$) and dielectric loss (tanδ) but KNN materials exhibits high ferroelectric properties at room temperature such as remanent polarization $P_r$(~8μC/$cm^2$), coercive field $E_c$(~11kV/cm), $P_{max}$(15μC/$cm^2$), $E_{max}$(30kV/cm). Potassium sodium niobates also show good optical properties and its energy band gap is approximately 3.62 eV [11-12].

### 1.5.2. Phase transitions of KNN Material

With the temperature change potassium sodium niobate shows phase transitions of crystal structure. When the temperature of a material varies from high to low then KNN ceramic exhibits phase transitions such as cubic to tetragonal, tetragonal to orthorhombic and orthorhombic to rhombohedral. Temperature range of phase transitions of KNN material shown in Figure 1.4.

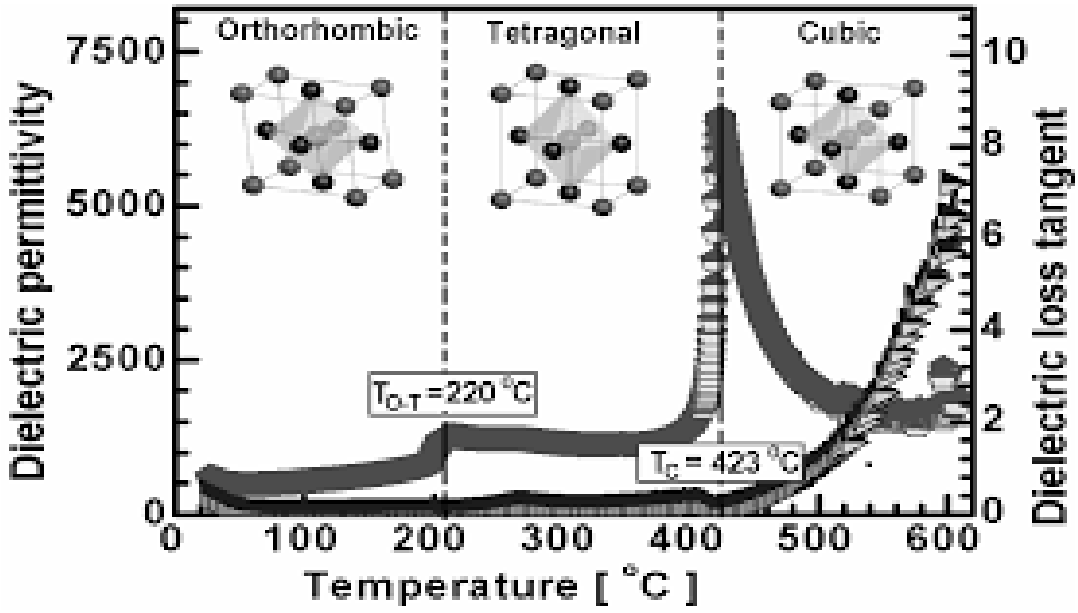


**Figure 1.4: Graph of Phase transitions of $K_{0.5}Na_{0.5}NbO_3$ ceramics [14].**

# *Chapter:2*
# *Literature Survey*

## 2. Literature Reviews

To enhance the properties of lead-free materials ( which are the alternative materials for lead-based material) researchers work on lead-free materials from some past years. First two highly researched lead-free materials were sodium bismuth titanate (NBT) and barium titanate (BT). These materials were used for the replacement of lead-based materials but NBT and BT materials exhibit poor piezoelectric and ferroelectric response as compared to lead contained materials. From 2004, researchers worked on new material such as potassium sodium niobate which gives the optimum results and this material exhibits good electromagnetic response which is compatible with a lead-based electromagnetic response.

In this section, we summarized the carried out research work on potassium sodium niobate material from some past and present years.

**ISHII et al., 2001** prepared a ceramics BNKT-100x which is solid solution of $(Bi_{1/2}Na_{1/2})\ TiO_3$ and $KNbO_3$ materials and these ceramics synthesized the conventional ceramic technique to investigate its structural and electrical properties. They were reported that (1-x) BNT-(x)KN solid solution exhibits coexistence of a rhombohedral and orthorhombic symmetries at room temperature. BNTK-100x also exhibits a wide range of resistivities from $10^9$–$10^{12}$cm and its unsaturated $K_{33}$ (electromechanical coupling factor) value was 0.16 [15].

**LINGWAL et al., 2003** prepared pure $KNbO_3$ and sodium(Na) doped $KNbO_3$ ceramics by ordinary sintering air technique and defined these ceramics with different characterization proficiencies i.e. SEM, XRD, dielectric studies. From this data, they were analyzed that dielectric properties decreased under frequency range from 10 KHz–1MHz, and temperature range from50–250°C. But dielectric conductivity increased as the rise in frequency. Near the transition temperature NKN ceramics exhibit anomalous behavior for dielectric properties. In these ceramics, dielectric loss and dielectric constant peaks shifted towards the lower temperature values at higher frequencies [16].

**Guo et. al., 2004** prepared the $(1-x)(K,Na)NbO_3–xLiTaO_3$ ceramics with solid-state reaction method. They were reported that (1-x)KNN-xLT solid solution exhibit perovskite structure

with orthorhombic symmetry when x<5mol% and changed into tetragonal symmetry when x>6. (1-x)KNN-xLT solid solution reveals the morphotropic phase boundary at x=5-6 mol%. But at x=8, (1-x)(K,Na)$NbO_3$–x$LiTaO_3$ ceramics begins to appear as a tungsten bronze structure with the tetragonal phase($K_3Li_2Nb_5O_{15}$). This solid solution shows ~200 pC/N $d_{33}$ value and~36% $K_P$ value. The higher piezoelectric properties of this solution show that it is promising lead-free material [17].

**Kosec et al., 2004** prepared (1−*x*) $K_{0.5}Na_{0.5}NbO_3$–*x*$SrTiO_3$ solid solution for composition x=0 to 0.33 by conventional mixed oxide route. They were reported that $K_{0.5}Na_{0.5}NbO_3$-$SrTiO_3$ ceramics exhibits lead-free relaxor behaviour and its relaxor properties increased with addition $SrTiO_3$ content into undoped KNN. Due to relaxor behaviour KNN-ST shows phase very small grain size, thin hysteresis loop, high recoverable energy storage density, and phase transitions at very low temperature[12].

**Guo et al., 2004** synthesized NKN-ST and NKN-BT ceramics by ordinary sintering technique to investigate its ferroelectric-relaxor behaviour. They reported that NKN-ST and NKN-BT ceramics got excellent relaxor behaviour and electromechanical properties such as piezoelectric constant $d_{33}$= 90-100 pC/N, electromechanical coupling cofficient $k_p$=32% and thickness coupling constant $k_t$=44%. They also observed that with addition of $BaTiO_3$ and $SrTiO_3$ content into NKN ceramics phase transition peaks were shifted at very low temperature values and peaks become much broader. NKN-ST ceramics shows much optimistic results than NKN-BT ceramics [18].

**Chang et al., 2006** prepared the samples of 0.95(K,Na)NbO3with the composition of 0.05 $AETiO_3$ (AE=Sr, Mg, Ba, Ca) ceramics and examined that pure KNN, KNN-ST, and KNN-CT depicts single perovskite phase but KNN-BT and KNN-MT exhibit secondary phase of ceramics. Pure KNN can be obtained good electromechanical properties ($K_P$=0.38, $d_{33}$=122pC/N, $\varepsilon_r$=421, $T_C$=406°C, tanδ=0.033) as compared to 0.95(K, Na)NbO3-0.05($AETiO_3$) Solid solution[5].

**Zuo et al., 2007** synthesized the lead-free piezoelectric ceramics which is a solid solution of (K, Na)$NbO_3$ and (Bi, Na)$TiO_3$ materials. This solid solution (KNN-BNT) at room temperature exhibits phase transitions due to different-different compositions and also shows morphotropic phase boundary (MPB) at x=0.02 to x=0.03. (1-x) (K,Na)$NbO_3$-x (Bi,Na)$TiO_3$ ceramics exhibits high coupling constant $k_p$(~43%) and high piezoelectric constant(~195 pC/N) near the morphotropic phase boundary and due to large Curie temperature along with the excellent electromechanical properties, it is promising lead free material[19].

**Wang et al., 2009** prepared ceramics of KNN doped with $BaZrO_3$ through the conventional ceramic route. They were analyzed potassium sodium niobate exhibit phase transitions such as cubic to tetragonal, tetragonal to orthorhombic, orthorhombic to rhombohedral at higher to lower

temperatures but these phase transitions show anomalous behavior due to addition of barium zirconate into potassium sodium niobate. In pure KNN ceramics, an orthorhombic-rhombohedral phase transition occurs at lower than room temperature but with doping of barium zirconate the same orthorhombic-rhombohedral phase transition occurs at higher than room temperature and this change in phase transition very optimum step for high-performance piezoelectric ceramics [20].

**Juárez et al., 2011** synthesized the (K, Na)$NbO_3$ piezoelectric ceramics by microwave-hydrothermal synthesis method. They were reported that ferroelectric domains in (K, Na)$NbO_3$ material with exaggerated grain growth through the SEM (scanning electron microscope) technique and mainly two types of ferroelectric domains are formed in KNN ceramics 180˚ and 90˚. 180˚ ferroelectric domain exhibited watermark pattern and its dimensions are 3–10 m width ×20–40 m length. 90˚ ferroelectric domain exhibited herringbone arrangement with *a–a* and a-c configurations and its dimensions are 0.5–1μm width×3–7μm length. 180˚ ferroelectric domain predominated by 90˚ ferroelectric domain [21].

**Wang et al., 2014** reported that alkali niobate-based system exhibits giant $d_{33}$ (∼490 pC/N) related to the rhombohedral-tetragonal phase boundary and wide performance of $d_{33}$ and $T_C$ could be achieved by optimal compositions of these alkali niobate systems and this good performance of $d_{33}$ enhances the electromechanical properties of these lead free materials. Due to gaint $d_{33}$, good electromechanical properties alkali niobate-based system are promising ceramics as an exchange of lead-based piezo-ceramics in the future [22].

**Wang et al., 2015** synthesized lead-free $BiFe_{0.8}Co_{0.2}O_3$ doped 0.95KNN-0.5KLS piezoelectric ceramics by mixed oxide route. From this solution analysis, they were examined that due to the content of $BiFe_{0.8}Co_{0.2}O_3$ changes occurred in structural, piezoelectric and ferroelectric properties of 0.95KNN-0.5LS polycrystalline materials. BFC content diffused into (K, Na) $NbO_3$ lattice and changed their lattice parameters. With the increase in BFC content, the grain size of solid solution (1-x)(KNN-LS)-x(BFC) becomes decreased and homogeneous. In solution (1-x)(KNN-LS)-x(BFC), Curie temperature $T_C$ decreased but peaks of $T_C$ becomes broaden. At $x<0.004$, this solution exhibits high $d_{33}$ (~276 pC/ N), high $k_p$ (52%) and more saturated P-E loops but at $x=0.004$, $k_p$ slightly decreased and material exhibits low remanent polarization and high coercive field [23].

**HARTTAR et al., 2015** reported that Alkaline niobate especially sodium potassiun niobate (NKN) materials are piezoceramics due to their high $d_{33}$ and $T_C$. But these KNN ceramics failed to achieve high-density structure and due to this reason intrinsic defects are formed in KNN ceramics. With the appropriate doping of rare earth metals, inherent intrinsic defects improved significantly and

the results indicate that rare earth metal doping in KNN ceramics enhanced the electrical properties of KNN based ceramics [24].

**Koruza et al., 2015** synthesized 0.85NKN–0.15STO ceramics by convention solid-state route and investigated the electrocaloric effect of 0.85NKN–0.15STO solid solution by direct method as a function of electric field and temperature. The Electrocaloric response of KNN-STO ceramics at 159 kV/cm is 1.2 K for 300K and 1.9 K for 340 K was measured in temperature limit of 80 K. These KNN-ST solid solutions are useful for dielectric cooling technologies[25].

**Liu et al., 2016** synthesized high quality $(1-x)K_{0.5}Na_{0.5}NbO_3–xSrTiO_3$ transparent ceramics for x=0.1 composition with pressure less sintering technique. These transparent ceramics prepared without using SPS and HIP sintering techniques. Bipolar strain of these ceramics exhibited fatigue-free behaviour. X-ray photon spectroscopy and impedance spectroscopy depicted less defect density of these ceramics and high fatigue-resistant property [26].

**Yang et al., 2016** fabricated lead free highly transmittance ceramics $(1–x)(K_{0.5}Na_{0.5})NbO_3–xLaBiO_3$ for concentration x=0.000, 0.005,0.010, 0.015, 0.020, 0.025, 0.040, 0.060 by solid reaction method to investigate effect of dopant $LaBiO_3$ content x on phase transitions, optical properties , electromechanical properties and micro structural properties. In this work, they were reported that KNN-LB ceramics has pseudo cubic phase structure, show 74% transmittance in visible spectra for x=0.25. They also found that relationship b/w transparency and relaxor behaviour [27].

**Su et al., 2016** prepared the NKN-ST (x=0-0.15) ceramics by conventional solid state method to identify its raman scattering properties and electromechanical properties. They were reported that that raman bands $\nu_5$ and $\nu_1$ of NKN-ST ceramics shifted at low wavelengths. With addition of large amount of $SrTiO_3$ content, these band become more wider and FWHM of $\nu_1$ band also increased which suggested order -disorder transformation. Dielectric study of NKN-ST ceramics exhibits the relaxor behaviour and TEM study of NKN-ST ceramics observed the liquid phase formation at x=0.08 [28].

**Gupta et al., 2017** examined the coexistence of positive and negative electrocaloric effect in $SrTiO_3$ doped (K, Na) $NbO_3$ polycrystalline ceramics through the indirect thermodynamic technique. At 40 kV/cm, negative and positive electrocaloric response get different-different values. The corresponding negative electrocaloric coefficient was $-0.24 \times 10^{-7}$ $K \cdot mV^{-1}$ at 273 K and positive electrocaloric coefficient was $0.7 \times 10^{-7}$ $K \cdot mV^{-1}$ at 333 K. due to these values of electrocaloric coefficient, material achieved the high recoverable storage energy density was 1.46 $J/cm^3$ and these results indicated that electrocaloric effect based materials are useful for

electrocaloric refrigeration and in electronic devices [29].

**Kumar et al., 2019** investigated the coexistence of positive and negative electrocaloric effect and recoverable energy storage density performance in (1-x)KNN-(x)LN ceramics for composition x=0.01, 0.03, and 0.05 by Maxwell's thermodynamic route. They reported that KNN-LN ceramics for composition x=0.01, 0.03, 0.05 exhibited high positive and negative electrocaloric effect, high recoverable energy storage density and energy storage efficiency[30].

# *Chapter:3*

# *Synthesis and Characterization Techniques*

## 3.1. Materials

1. To synthesize the KNN, KNN-ST (10) and KNN-ST (20) ceramics with conventional solid state ceramic method.
2. To study the effect of doping of $SrTiO_3$ ceramics and study the properties of these ceramics.

## 3.2 Synthesis

### 3.2.1 Solid state ceramic route

Solid state route is a dried powder technique that is commonly used in material science research. Though this method, we can synthesize the polycrystalline ceramics. At the starting of this method, metal oxides, and carbonates, etc. are weighed through the micro-balance according to the stoichiometric formula of compounds. These metal oxides and carbonates commonly are fine-grained powdered chemicals that are after weighing, mixed and grind through the agate-motor in wet media(distilled water or acetone) to make the fine and homogeneous mixture. Grinding and mixing reduce the particle size of precursors. After this step, on these precursors solid state reaction takes place and that reaction is known as calcination or firing which is heat treatment which makes a homogenous body of precursors at a particular temperature. The next step is pelletization, in which disk-shaped pallets(polyvinyl-alcohol mixed powdered disks) of calcined powder are formed through the hydraulic press and these pellets are densified by sintering process which is also a heat treatment to control shrinkage of sample materials. At the end of this method, these sintered pellets are painted with the silver paint to make the electrodes and after electrode, these pellets are used to identify the sample material's electromechanical properties [31].

### 3.2.2 Sample preparation of KNN and KNN-ST ceramics

Pure $(K,Na)NbO_3$ and $SrTiO_3$ doped $(K,Na)NbO_3$ based ceramics synthesized through the solid-state ceramic method and for the experimental procedure some raw materials were used such as potassium carbonate($K_2CO_3$) with 99% purity, sodium carbonate($Na_2CO_3$) with 99.95-100.05% purity, strontium carbonate($SrCO_3$) with 99% purity, niobium pentaoxide($Nb_2O_5$) with 98% purity, titanium dioxide($TiO_2$) with 99.9% purity, acetone and distilled water. Experimental procedure of KNN and KNN-ST ceramics as follows here:

Firstly for pure $(K,Na)NbO_3$ ceramics, raw materials $K_2CO_3$,$Na_2CO_3$ and $Nb_2O_5$ weighed according to stoichiometric formula of their compounds through the micro-balance machine and after weighing of these materials, the powder of these precursors was ground in agate motor for 8-10

hours to obtain the fine ground powder which is essential to control the particle size and make the homogenous body of precursors. So the obtained fine ground powder' s calcination temperature was at 900˚C (2hours) in the tabular furnace. After calcination, some amount of powder was used for XRD analysis and some amount of powder was used to making disk-shaped pallets ( powder compacts were pressed at 100MPa) through the hydraulic press. Pellets were sintered at 1100˚C for 2hours in the tabular furnace for densification of samples and after those disk-shaped pallets were polished by electrically conducting silver paint to make pallets as electrodes. In the end, these silver painted pallets were used for electro-mechanical observations. Figure 3.1 shows the flow chart of the preparation of pure KNN ceramics.

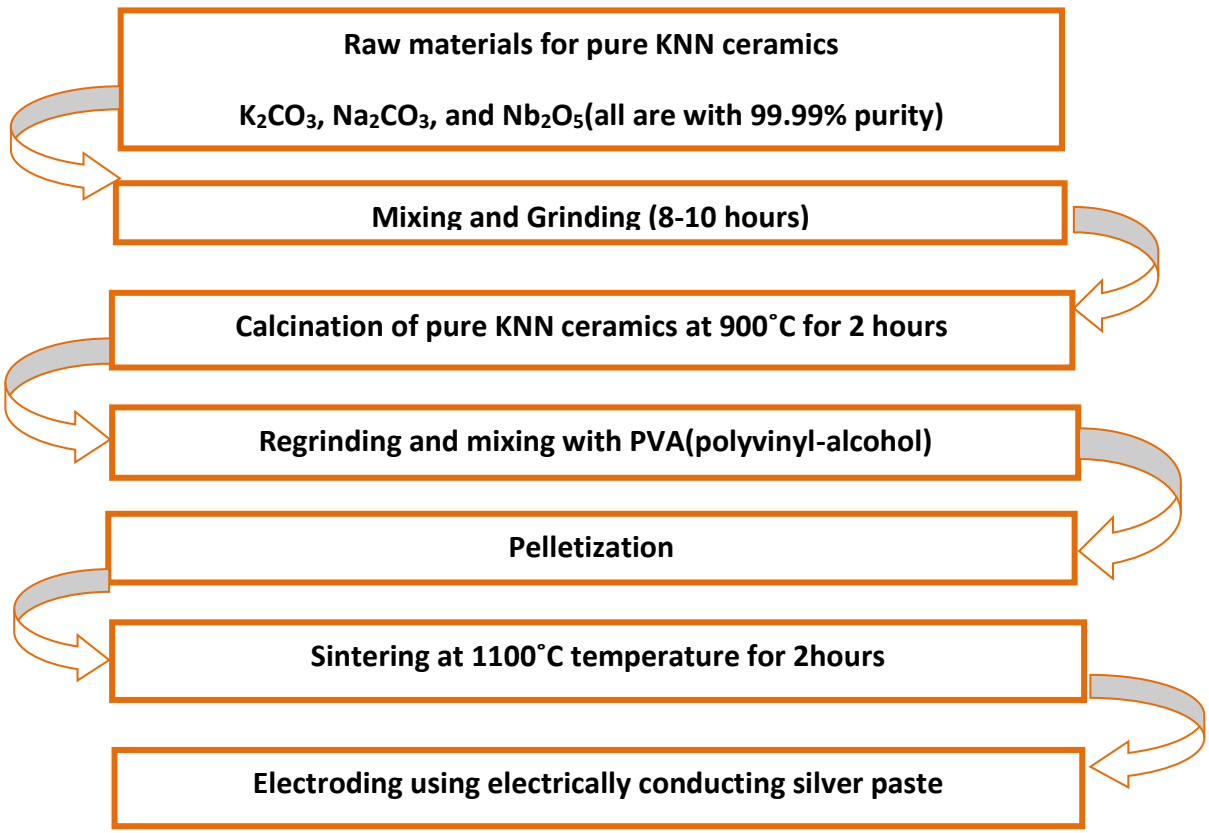


**Figure 3.1: Flow chart of synthesis of pure KNN ceramics by solid state route**

Secondly, 0.9KNN-0.1STand 0.8KNN-0.2STceramics were synthesized by the solid-state route and first of all raw materials given above K2CO3, Na2CO3, Nb2O5, SrCO3, and TiO2 were weighed with a suitable amount and the powder was ground and mixed for 8-10 hours in agate motor. The ground powder's calcination temperature was 900˚C(2 hours) in tabular furnace. Small amount of calcined powder used for XRD analysis and some amount of powder compacts were uni-axially pressed under 100MPa pressure in hydraulic press named instrument. These pellets were sintered at a 1200˚C temperature in tabular furnace. The pallets were painted with electrically conducting

silver paint for electrode and these pallets were used for dielectric studies, piezoelectric studies, and ferroelectric studies. Fig. shows that flow chart of preparation of 0.9KNN-0.1STand 0.8KNN-0.2ST ceramics.

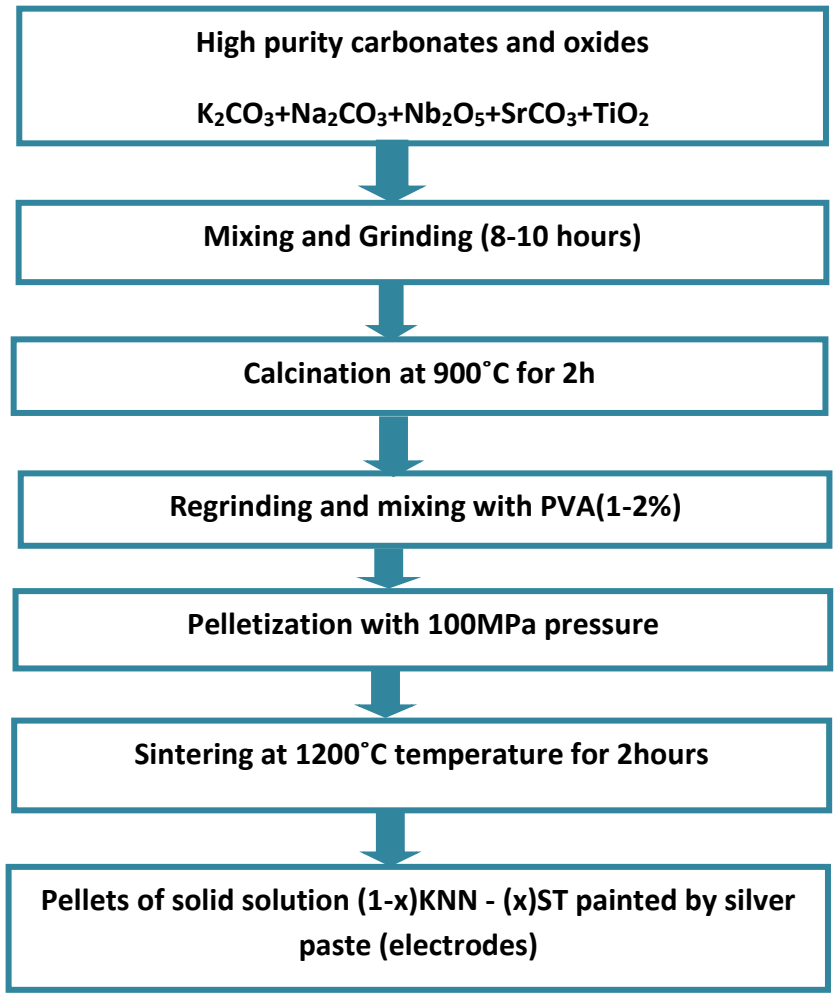


**Figure 3.2: Flow chart of synthesis of $SrTiO_3$ doped KNN ceramics**

## 3.3. Characterization Techniques

### 3.3.1. X-ray diffraction

It is the non-destructive technique used to determine the properties of a crystalline material and it transmits information on the lattice structure dimensions.

**Principal and Instrumentation**

X-ray diffraction is presently a typical system for the investigation of atomic spacing & crystal structure. X-ray diffraction mostly depends on valuable obstruction of monochromatic x-rays & crystalline samples. The association of the x-ray with the sample produces helpful obstruction and diffraction rays when conditions fulfill Bragg's law and lattice symmetry.

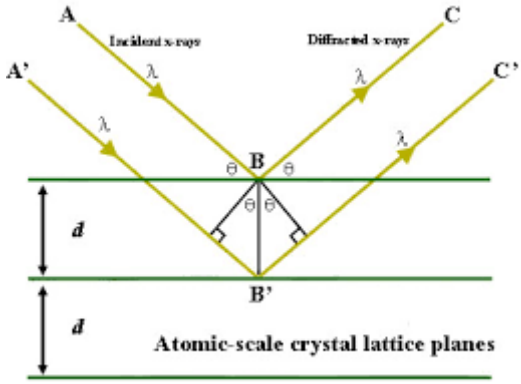


**Figure 3.3: Schematic diagram of bragg's law**

$$2dsin\theta = n\lambda \ldots (1)$$

Here,

**d= inter atomic spacing**

**λ= wave-length of x-rays**

**n= intger value**

In the literature reported that KNN shows orthorhombic symmetry which is calculated by formula:

$$1/d^2_{hkl} = (h^2/a^2+k^2/b^2+l^2/c^2)\ldots\ldots\ldots(2)$$

and SrTiO3 doped KNN ceramics exhibits tetragonal symmetry which is calculated by formula:

$$1/d^2_{hkl} =[h^2+k^2+l^2(a/c)^2]1/a^2\ldots..(3)$$

X-ray diffractometer comprises of three fundamental sections: an x-ray tube, sample holder and x-ray indicator. X-rays are created in a cathode x-ray tube by warning a fiber to deliver electrons, quickening the electrons toward an objective by applying a voltage and assaulting the objective material with electrons. At the point when electrons have adequate vitality to oust inward shell electrons of the objective material, a trademark x-ray spectrum is delivered. These spectra comprise

of a few segments, the most widely recognized being kα and kβ. These x-rays are collimated & coordinated onto the sample, as an x-ray is recorded. At the point when the geometry of the x-ray impinging the sample fulfills the Bragg's equation. The particular wavelengths are normal for the objective material (Fe,Cu and Mo). Copper is the most well-known target material for single-crystal diffraction, with Cu Kα radiation= 1.5418 Å. For the structural analysis we also used x-ray diffractometer of model Panalytical. X.Pert pro with copper radiation Kα from SAIF department PU, Chandigarh.

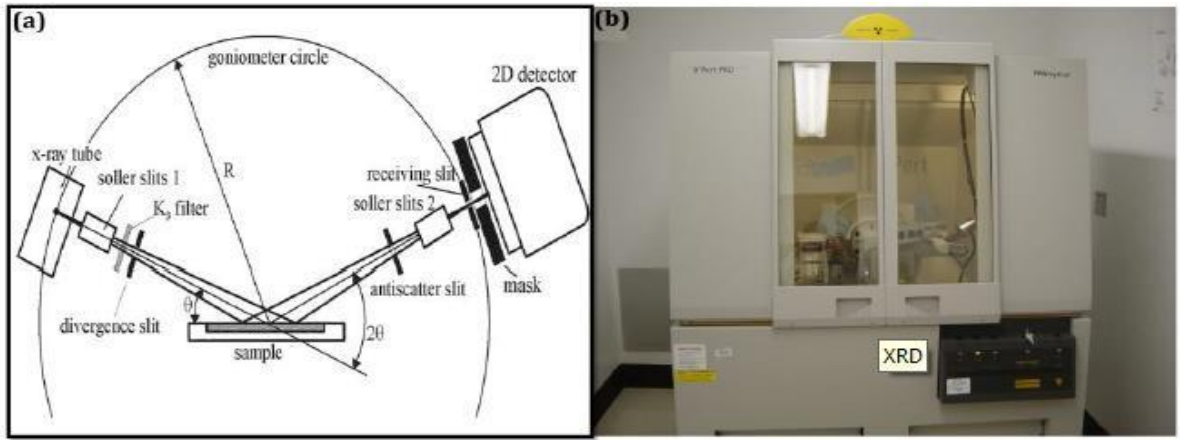


**Figure 3.4: shows (a). The geometry of goniometer (b). X-ray diffractometer**

**Sample Preparation**

For the measurement, we need finely ground powder. While putting the powder in the sample makes sure the powder is well-settled at the bottom of the sample holder, to get the appropriate results [9].

**3.3.2 SEM**

It is an electron type microscope that scans the sample surface with electrons occupied focused beam. The information regarding the sample's composition & topography of the surface is obtained by the production of various signals when there is an interaction of electrons with atoms. An image is obtained when the intensity of the detected signal combines with the beam's position and the pattern under which the beam is scanned is called a raster scan. During semiconducting it's important to laminate the sample using thin gold foil or palladium alloys containing gold or use carbon so that the sample can conduct electricity. Observation of SEM specimens depends on the environment and pressure of SEM, it should be observed in low vacuum, high vacuum or wet condition. For the microstructural analysis of KNN and KNN-ST ceramics we used SEM model JEOL JSM-6510LV from SAI labs TIET Patiala.


**Figure 3.5: SEM instrument**

### 3.3.2.1 EDX

The energy dispersive spectroscopy is surface analytical proficiency which is used to recognize the elemental composition of samples and energy dispersive spectroscope is a part of SEM instrument which uses x-rays for identification of elemental compositions. It can identify all elements of periodic table from 4(Be) to92(U). Energy dispersive spectroscope is an integrated part of scanning electron microscope which is consists of liquid nitrogen dewar,x-ray detector, an electron gun.

**Sample preparation**

In case of non-conducting ceramics, sintered pellets firstly coated with gold thin layer by sputter coating for some time and after that when ceramics start conducting placed into scanning electron microscope for analysis.


**Figure 3.6: EDX Instrument**

### 3.3.3. Dielectric Measurement.

A dielectric ceramic is an electric insulator that can be polarized by an applied electric field. The dielectric constant of a material is given as:

$$\varepsilon_r = (C/C_O) \quad \text{.....(4)}$$

$$C_O = \varepsilon_o(A/d) \quad \text{.....(5)}$$

$$C = (\varepsilon_r\varepsilon_o)A/d \quad \text{.....(6)}$$

Here

**A= area of two parallel plate capacitors**

**d= distance between two parallel paced capacitors**

**Instrumentation & working principle**

For a typical LCR meter, these measurements are done based on the automatic balancing bridge route. Here, the impedance of the device can be calculated from Resistance [32]. For the dielectric & impedance study of KNN and KNN-ST ceramics we used LCR meter model no. PSM1735 from SMART material lab TIET Patiala.


**Figure 3.7**: **LCR meter and balancing bridge instrument**

**Sample preparation**

- Finely grounded powder including polyvinyl alcohol (PVA) which acts as a binder.
- This grounded powder is compacted to get .10mm in dia. & 1mm thick cylindrical pallets.
- The cylindrical pellets are sintered at 500˚C and to form contacts, silver paste coating is done on their circular surfaces[32].

### 3.3.4. P-E loop measurement

Polarization is a phenomenon that occurs when the positivity & negative charges of material get displaced in directions towards the opposite units of an applied electric field, due to which local dipoles are created inside that material and this moment of dipoles in that volume is called as polarization.

There are many ways which result in polarization in a material stated as follow:-

**Space charge polarization: -** It is defined as the accumulated charges at an electrodes due to their limited motion. Therefore, we can say that it is a sum of all other contributions from many other sources.

**Orientation polarization: -** It is seen electro-negatively different molecules such as $CH_3CI$ which means even in the absence of electric field they show dipole moment, but in the presence of electric field these molecules align themselves in its direction, this change of molecule aligning themselves results in orientation polarization.

**Electronic polarization: -** It is observed on the application of electric field, displacement of nucleus & the electron occurs in a direction away from each other in an atom. In all this, the strength of the applied electric field determines extent of displacement.

**Ionic polarisation:** - It is seen when the ions in the ionic solids shift with respect to the other opposite charged ions. As in this shift of electrons cloud similar to the nucleus appears different from electronic polarization [31-32].

**Instrumentation & working princip**le

Based on the Sawyer-Tower circuit and using P-E loop tracer the ferroelectric measurements were calculated. This method is simple to be implemented. The charge on two capacitors is the same when connected in series. The components that are used in the Sawyer-Tower circuit are as follow: -

- Ferroelectric sample
- Function Generator
- Oscilloscope
- Two capacitors

The oscilloscope axis (x & y) demonstrates potential over standard capacitors when a voltage is generated by the function generator.

$$V = (Q / C) \quad \textbf{.....(4)}$$

Here

**Q= electric charge of sample material.**

**C= Capacitance of sample material.**

We have done ferroelectric measurements from at Automatic PE Loop Tracer model of MARINE INDIA.

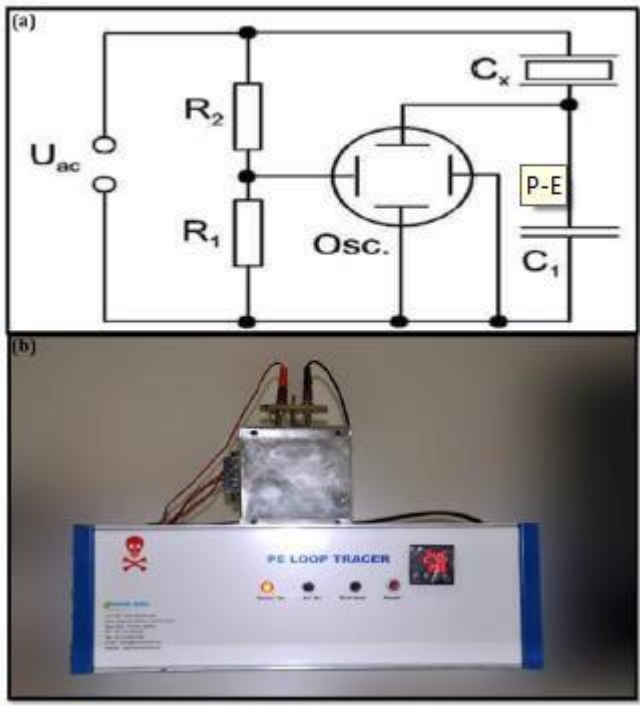


**Figure 3.8: shows (a) circuit diagram of P-E loop tracer(b) P-E loop tracer instrument.**

### 3.3.5 UV-Visible Spectroscopy

Ultraviolet-visible spectroscopy is an absorption spectroscopy which works under ultra-violet and visible spectral regions. Ultra violet-visible spectroscopy is observation of attenuation of light after passing through sample but sometimes light can reflects from sample's surface. Absorption measurements used only monochromatic wavelengths.

**Principal and Instrumentation**

UV-visible spectroscopy based on Lambert and Beer-Bouguer law and this law states that when beam of light passes through the solution then attenuation in light's intensity is directly proportional to concentration of solution and light intensity. Optical analysis done by UV Spectrometer model no. from Nano Medicine Lab Patiala.

Components of UV-Visible Spectrophotometer

- Mono-chromator
- Detector
- Recorder
- Source
- Sample Compartment


**Figure 3.9: UV-visible spectrophotometer instrument**

# *CHAPTER:4*
# *RESULTS AND DISCUSSIONS*

## 4.1. Overview

This chapter is a very important part of this thesis report. This chapter includes the results and discussions of experimental work of pure KNN and KNN-ST ceramics. In this chapter, we described phase structure of crystalline KNN, KNN-ST(10), and KNNST(20) ceramics through XRD technique, ferroelectric response of ceramics with P-E hysteresis technique, description of microstructure (like grain, grain boundaries) with SEM, and dielectric studies with LCR technique. These results are discussed below.

## 4.2 X-ray diffraction studies

Figure 4.1(a) shows room temperature XRD patterns of KNN, KNN-ST(10) and KNN-ST(20) ceramics. XRD pattern of KNN clearly exhibits no impurity peaks or secondary phase and all the peaks correspond to orthorhombic structure as confirmed by ICDD standard card (ICDD card no. 71-2171). With the content of SrTiO3, orthorhombic phase gets transformed into perovskite tetragonal phase with space group *P433*. It is confirmed from ICDD card no.-71-0945. Since no extra peak of $SrTiO_3$ is evident, it is confirmed that $SrTiO_3$ has completely diffused into $(K,Na)NbO_3$ solid solution. This structural transformation is more evident from zoomed in view of the XRD pattern in 2θ range from 43˚ to 47˚as shown in Figure 4.1(b). The splitted peaks of KNN merged into single peak [12].

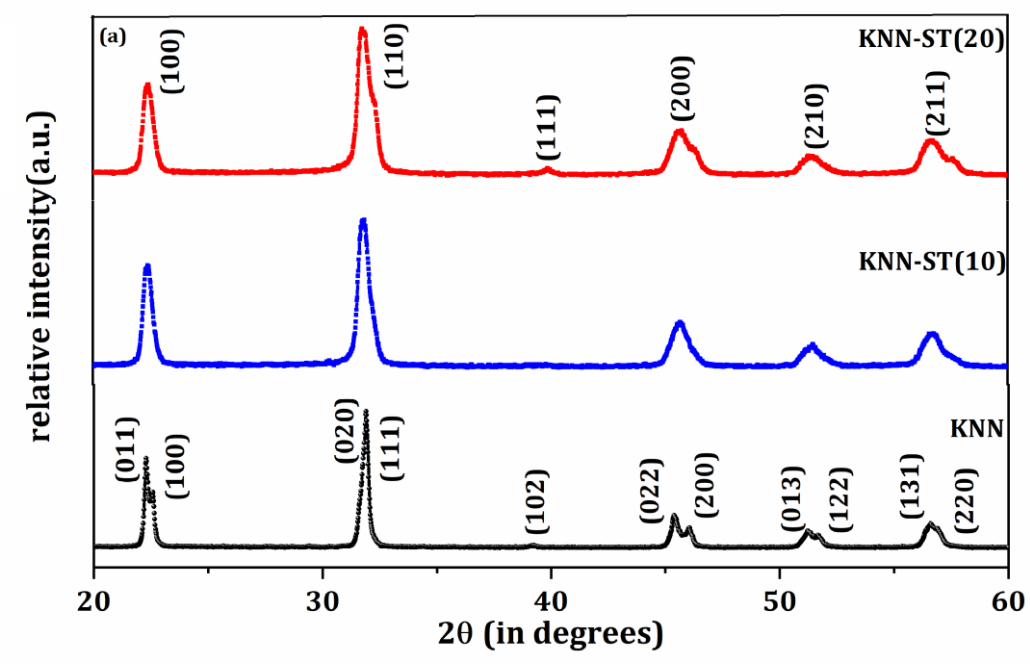


**Figure 4.1:(a) XRD pattern of (1-x) KNN (x) ST solution with Composition x=0, 0.1, 0.2**

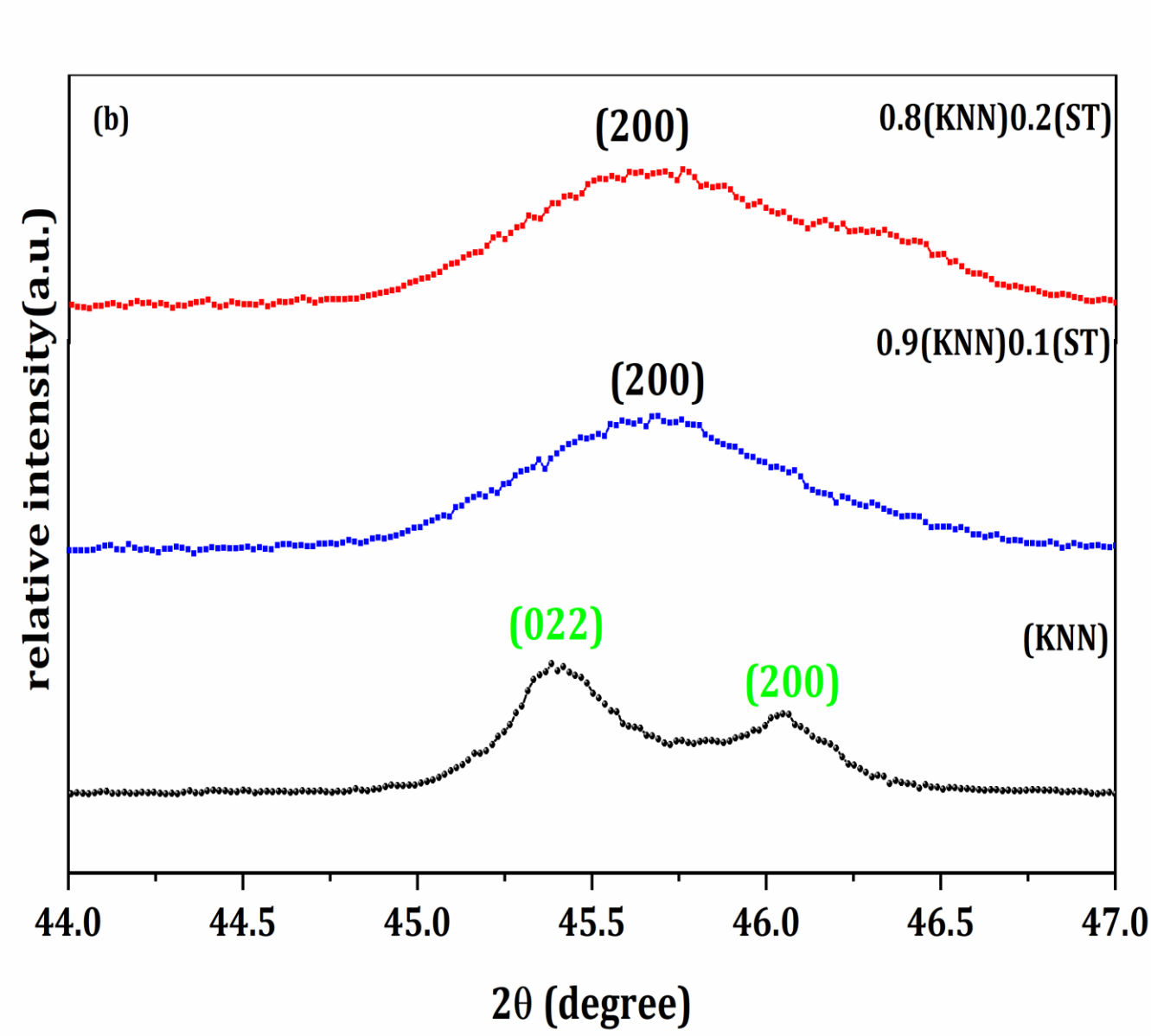


**Figure 4.1(b) Zoomed view of XRD pattern of (1-x) KNN-(x) ST with composition x=0, 0.1, 0.2 in 2θ range 44˚ to 47**

Lattice parameters of undoped KNN and SrTiO3 doped KNN unit cell (shown in Table 4.2).

**Table 4.1: Lattice parameters of (1-x) KNN- (x)ST solution**

| Compositions (x) | Lattice Parameters (Å) | | |
|---|---|---|---|
| | a | b | c |
| KNN | 3.9806 | 5.6022 | 5.3826 |
| KNN-10ST | 3.9630 | 3.9630 | 3.9540 |
| KNN-20ST | 3.9534 | 3.9534 | 3.7769 |

But with increasing the content $SrTiO_3$ into ceramics peaks of (1-x)KNN-xST solution is more broaden(shown in Figure 4.1 (a) and Figure 4.1(b) and lead free bulk ceramics are transformed in lead free relaxor ferroelectric ceramics.

It is noticeable that ionic radii of $Sr^{2+}$(0.144nm) similar to $Na^{1+}$(0.139nm) and $K^{1+}$(1.64nm) but $Ti^{4+}$ionic radius(0.061nm) is similar to $Nb^{5+}$ionic radius (0.064nm).So $Sr^{2+}$ ions could substitute for $K^{1+}$ and $Na^{1+}$, while $Ti^{4+}$ions could substitute for$Nb^{5+}$ions[33].

## 4.3 Micro structural studies

Figure4.2 shows the surface morphology of all (1-x)KNN-(x)ST solid solutions with composition x=0, 0.1, 0.2. Figure4.2 (a) depicts micro structure of undoped KNN in which large square shaped grains, polygon shaped pores and grain boundaries are present. Figure4.2 (b) exhibits the micro structure of KNN-ST(10) ceramics which shows submicrometer scaled grains with large amount of porosity. Figure4.2(c) exhibits microstructure of KNN-ST(20) solid solution. Micro structure of KNN-ST(20) is dense microstructure in which very small sized grains (at submicronmeter scale) are present with some porosity. Micro structural studies of (1-x)KNN-(x)ST solid solution exhibited that large sized grains of undoped KNN transformed into submicrometer scaled grains with doping of $SrTIO_3$ material and this occurred due to phase transformation of orthorhombic to tetragonal symmetry and with increasing the content of $SrTiO_3$.These micro structural results are very optimistic because with decrease in grain size of (1-x)KNN(x)ST solution dielectric breakdown strength(DBS), recoverable electric energy density(*Wrec*) and energy storage efficiency should increased[34].

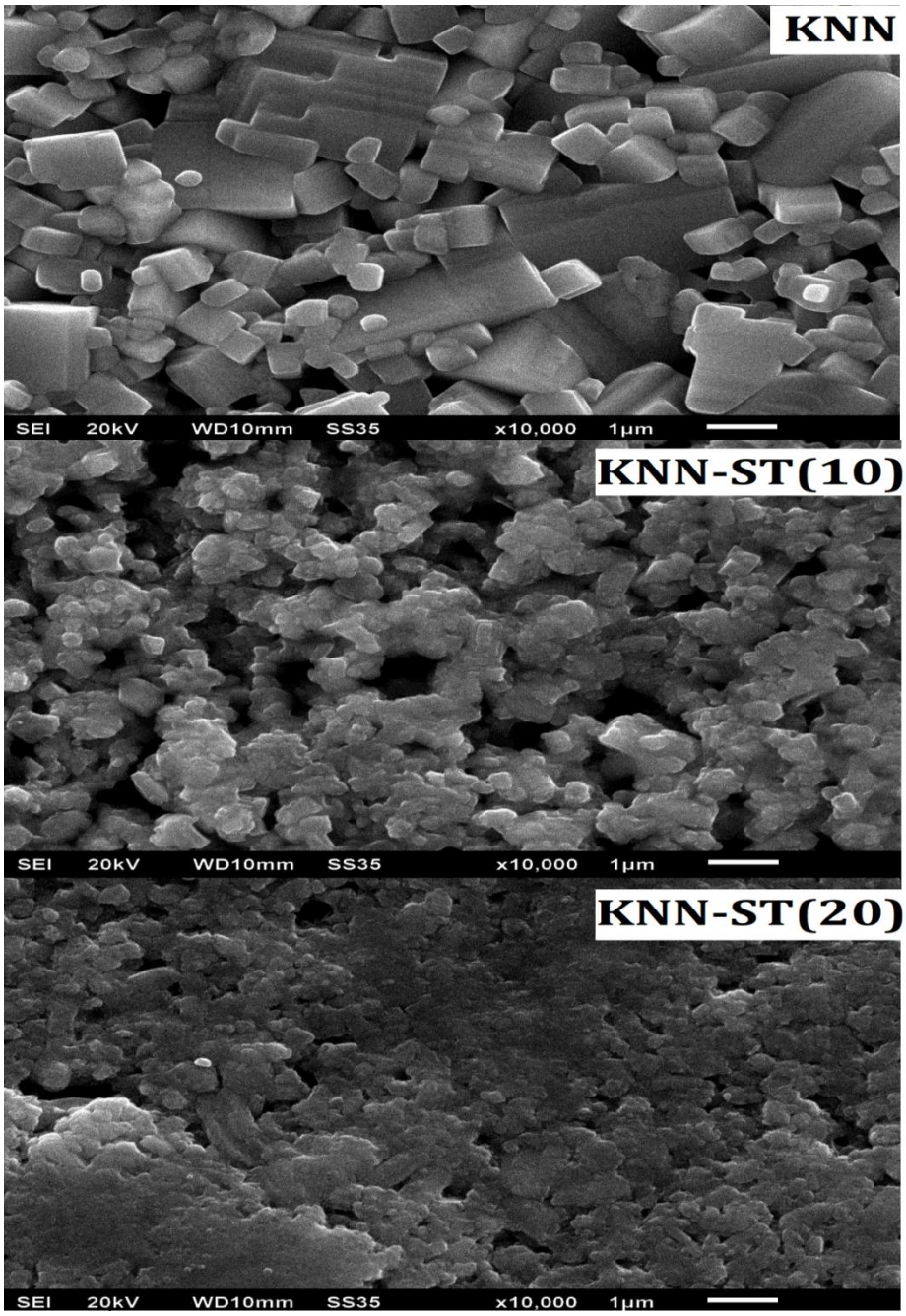


**Figure 4.2: SEM micrograph (a)undoped KNN (b) KNN-ST(10) (c) KNN-ST(20)**

**Energy dispersive spectroscopy**

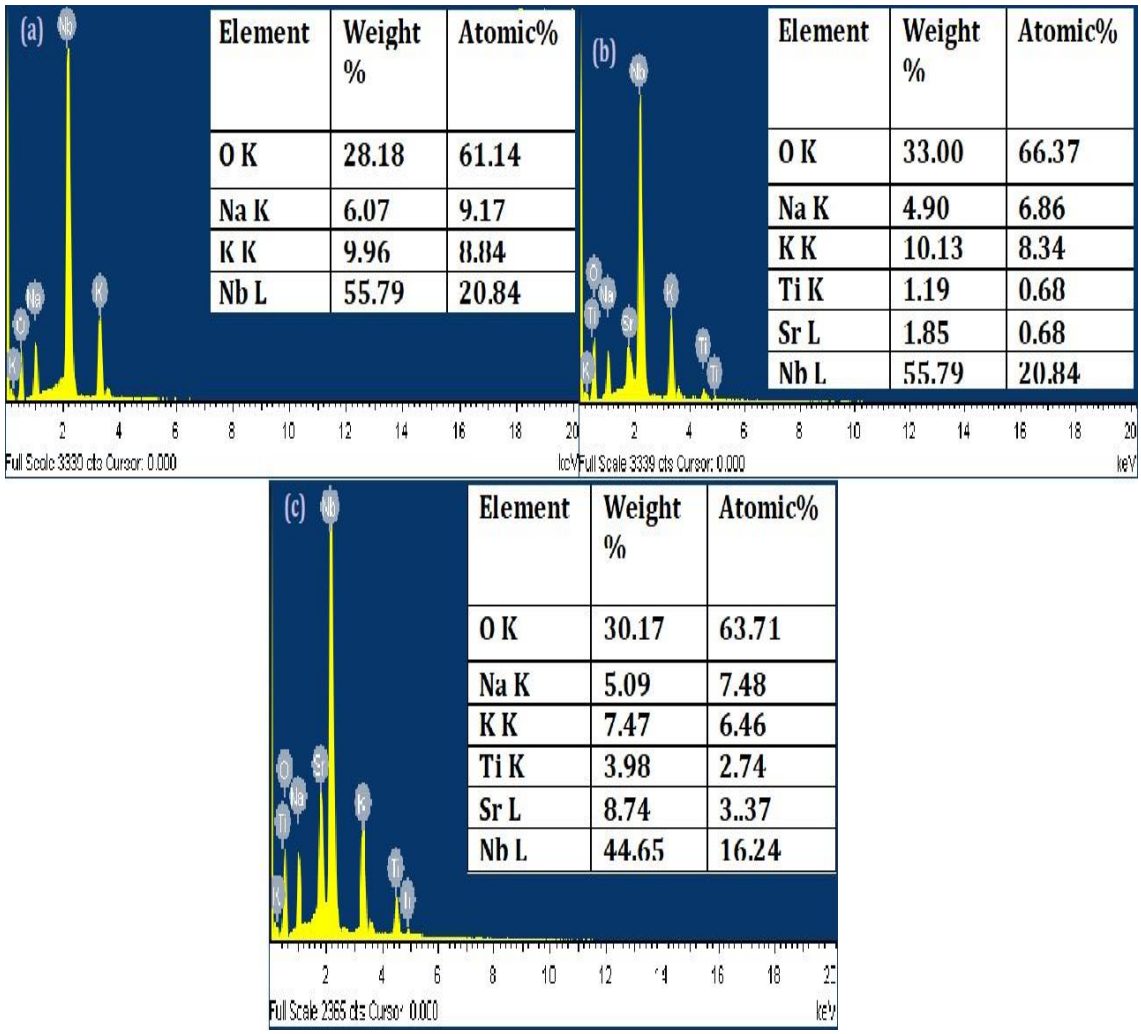


**Figure 4.3: EDX pattren of (a) KNN (b) KNN-ST(10) (c) KNN-ST(20)**

Fig.4.3 exhibits the EDX patterns of undoped KNN and $SrTiO_3$ doped KNN. It shows similar elemental distribution as taken initially.

## 4.4. P-E hysteresis loop studies

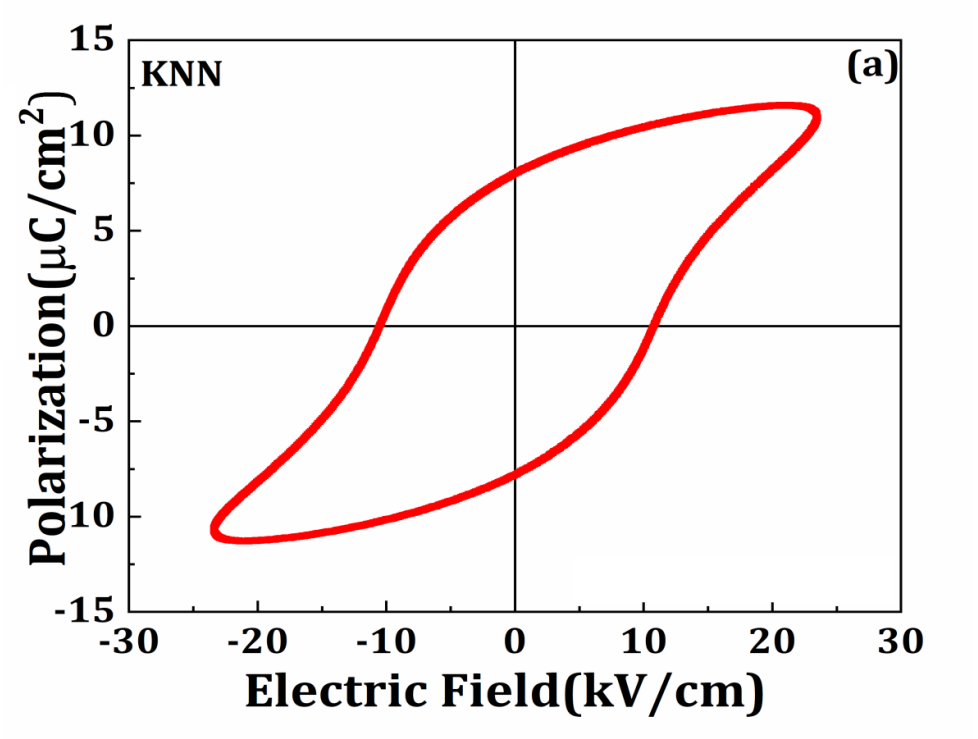


**Figure 4.4(a): P-E hysteresis loop of undoped KNN ceramics**

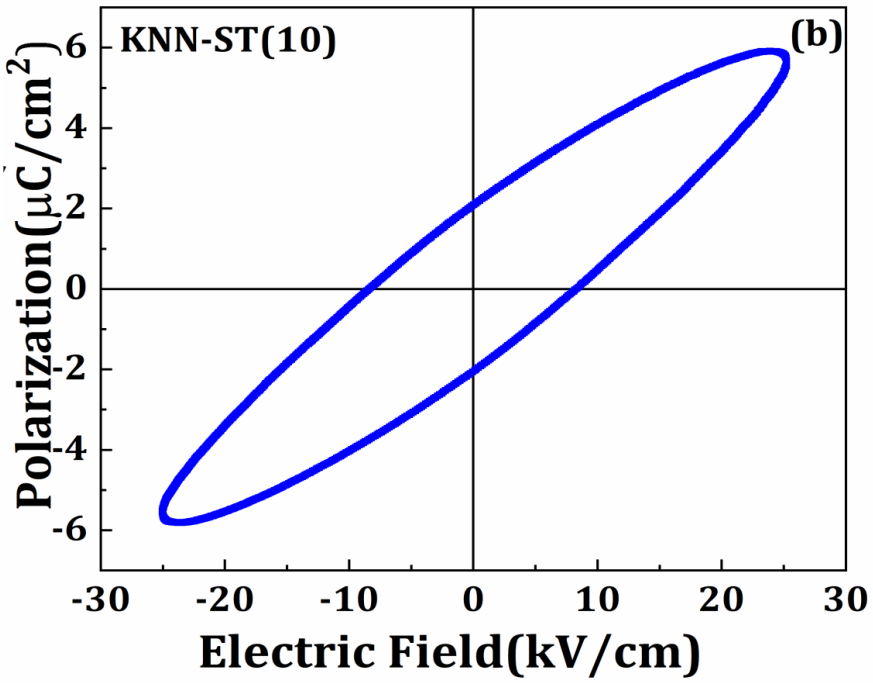


**Figure 4.4(b): P-E hysteresis loop of KNN-ST(10) ceramics.**

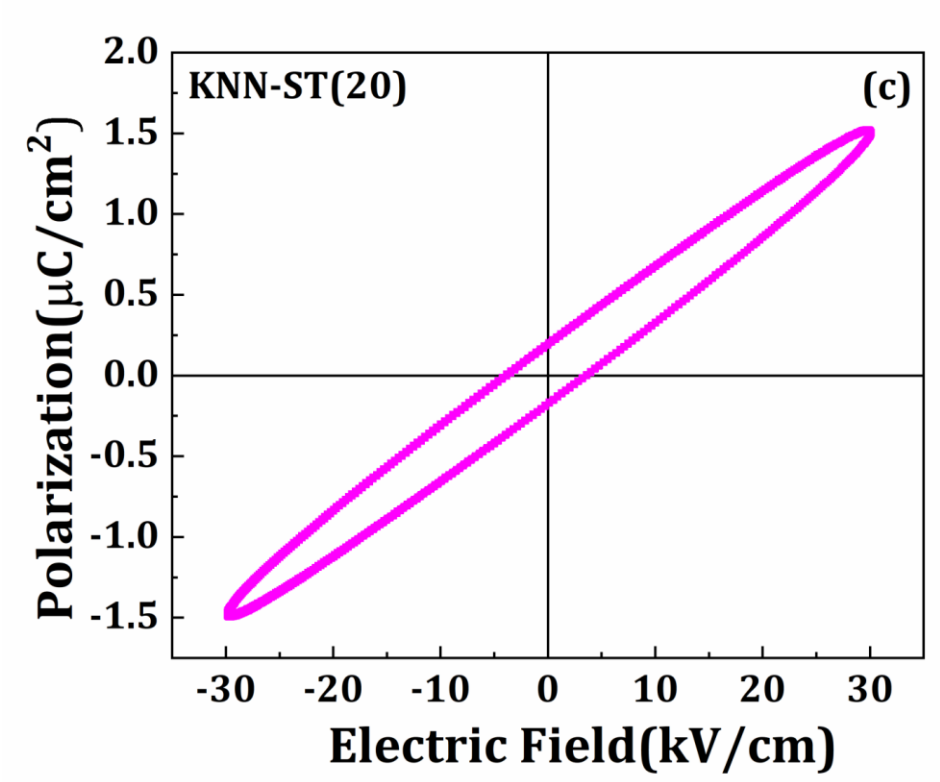


**Figure 4.4(c): P-E hysteresis loop of KNN-ST(20 ) ceramics**

Figure 4.4(a), (b), &(c) depict the P-E ferroelectric loops for undoped KNN and $SrTiO_3$ doped KNN with compositions x=0.1, 0.2 at 14kV/cm electric field value. P-E loop for undoped KNN shows high polarization value with appropriate shape of hysteresis loop. On the other hand with addition of $SrTiO_3$ (i.e. x=0.1and x=0.2), thin hysteresis loops have been found as shown in Figure 4.4(b) & 4.4(c). The remanent polarization ($P_r$), maximum polarization ($P_{max}$) and coercive field ($E_c$) for all the compositions are tabulated in Table 4.3. Decreases in case of (1-x) KNN-(x) ST (i.e. x=0.1and x=0.2) ceramics but maximum field ($E_{max}$) increases.

The result represents that ferroelectric properties of (1-x) KNN-(x) ST ceramics are weekend upon adding $SrTiO_3$. This behavior may be attributed to two reasons. First, $SrTiO_3$ ceramics behave non ferroelectric behaviour at room temperature and another with addition of $SrTiO_3$ content phase structure of (1-x) KNN-(x) ST change orthorhombic to tetragonal. Due to thin P-E hysteresis loop in case of (1-x)KNN-(x) ST ceramics (x=0.1,0.2) energy storage density becomes high and energy storage loss decreases similar to earlier reports [35].

**Table 4.2: P-E hysteresis loop parameters of (1-x)KNN-(x)ST solution**

| Composition (x) | Ferroelectric loop parameters | | | |
|---|---|---|---|---|
| | $P_r$(μC/cm$^2$) | $E_c$(kV/cm) | $P_{max}$(μC/cm$^2$) | $E_{max}$(kV/cm) |
| KNN | 7.907 | 10.654 | 11.430 | 23.458 |
| 0.9KNN0.1$^{ST}$ | 2.068 | 8.332 | 5.863 | 25.133 |
| 0.8KNN0.2ST | 0.182 | 3.696 | 1.436 | 29.293 |

## 4.5. Dielectric Studies

Temperature dependent dielectric constant (ε') and dielectric loss (tanδ) of (1-x)KNN-(x)ST solution for(x=0, 0.1, 0.2) at different-different frequencies are shown in figure4.5, 4.6(a) & (b). Dielectric graph of undoped KNN exhibits two peaks of dielectric constant at different temperature values. First peak is present at 230˚C (transition temperature $T_d$) and second peak is present at 430˚C (Curie temperature $T_c$). Above transition temperature, orthorhombic phase of KNN is transformed into tetragonal phase and above Curie temperature $T_C$, tetragonal phase is transformed into cubic phase.

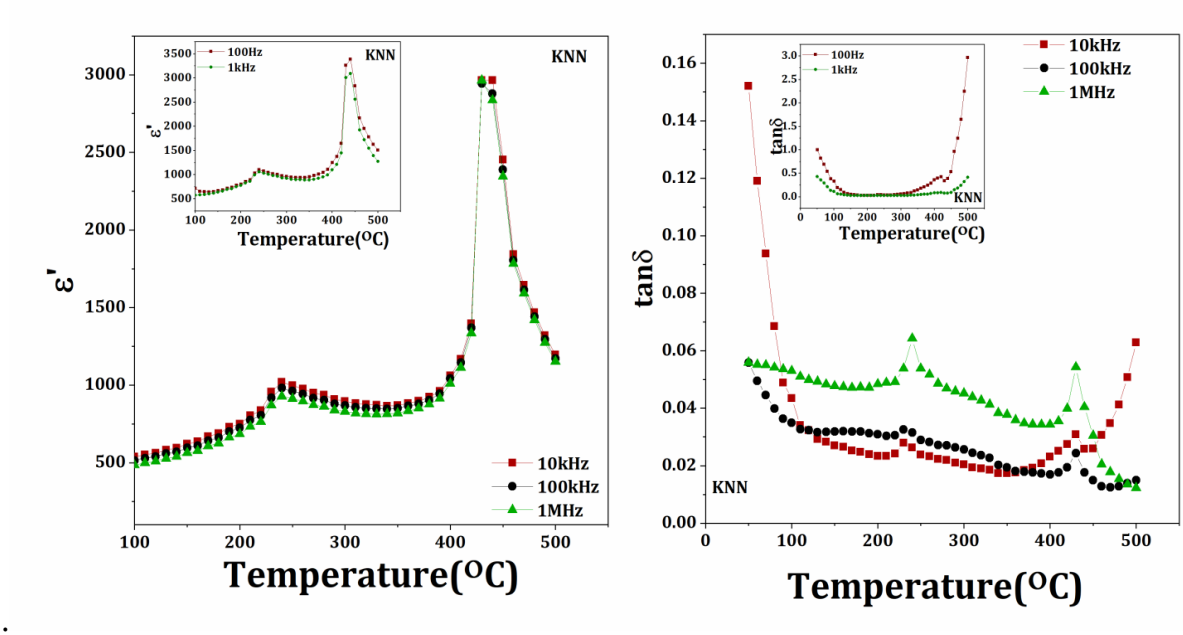


**Figure 4.5: Representation of dielectric study of KNN ceramics, inset shows variation in dielectric study at low frequency**

Dielectric graph of KNN-ST (10) (Figure 4.6(b)) represented that phase transition peaks shift at 188˚C from 430˚C and become more broader.

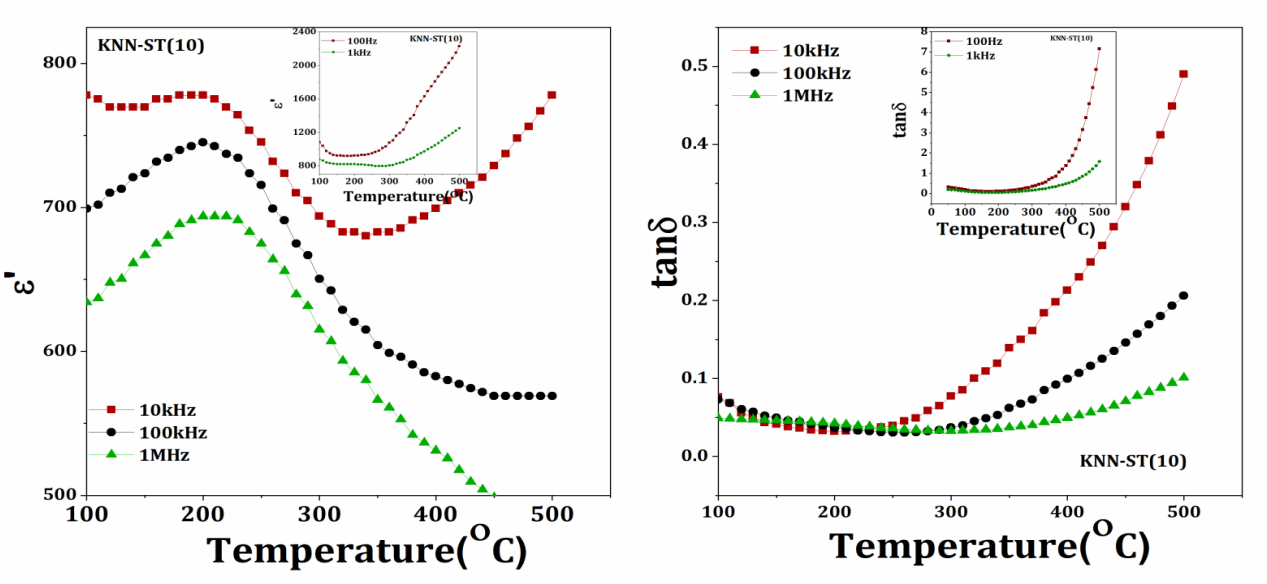


**Figure 4.6(a):Represents of dielectric study of KNN-ST(10) ceramics at higher frequency, the inset shows variation in dielectric study at low frequency**

and dielectric graph of KNN-ST(20)(figure4.6(c)) represented that phase transition peak shifted at very low temperatures so no any phase transition peak is visible in the temperature range from 100˚C to 500˚C

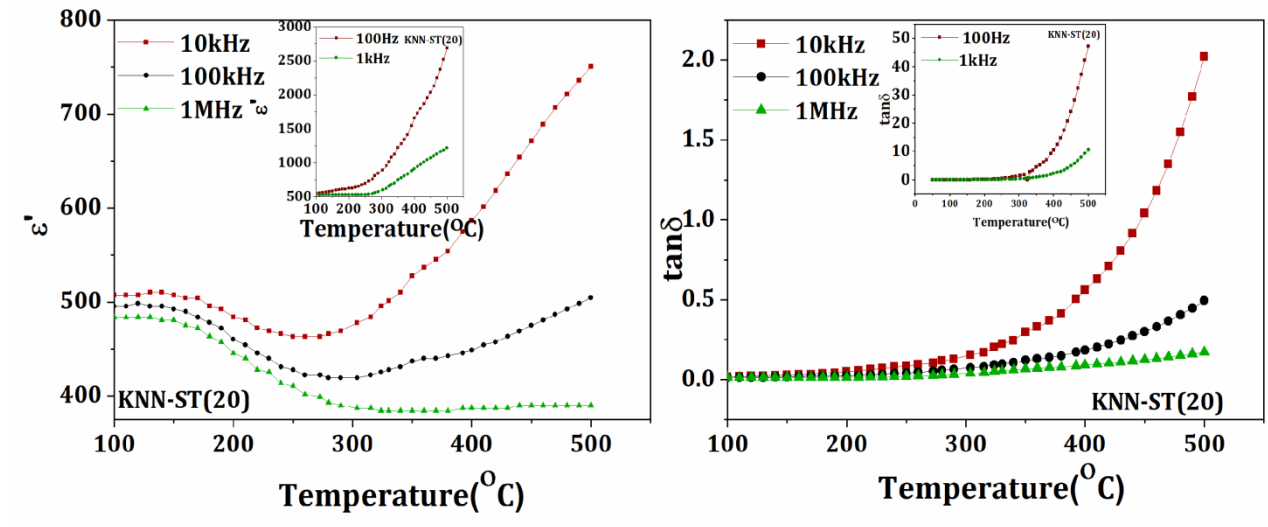


**Figure4.6(b): Represents of dielectric study of KNN-ST(20) ceramics at higher frequency, the inset shows variation in dielectric study at low frequency**

With addition of $SrTiO_3$ content into KNN, ceramics exhibit relaxor character and dielectric breakdown strength is increased. Figure4.7 exhibits the variation of dielectric constant (ε') and

dielectric loss (tanδ) for KNN, KNN-ST (10), and KNN-ST(20) solid solution as a function of frequency at various temperatures. Both values ε' and tanδ increased with doping of $SrTiO_3$ at lower frequencies but at higher value of frequency ε' and tanδ decreased and then remain constant at very high frequency values for undoped KNN. Values of ε' and tanδ, at 100Hz and 1kHz for KNN-ST (10) and KNN-ST(20) greater than KNN [36].

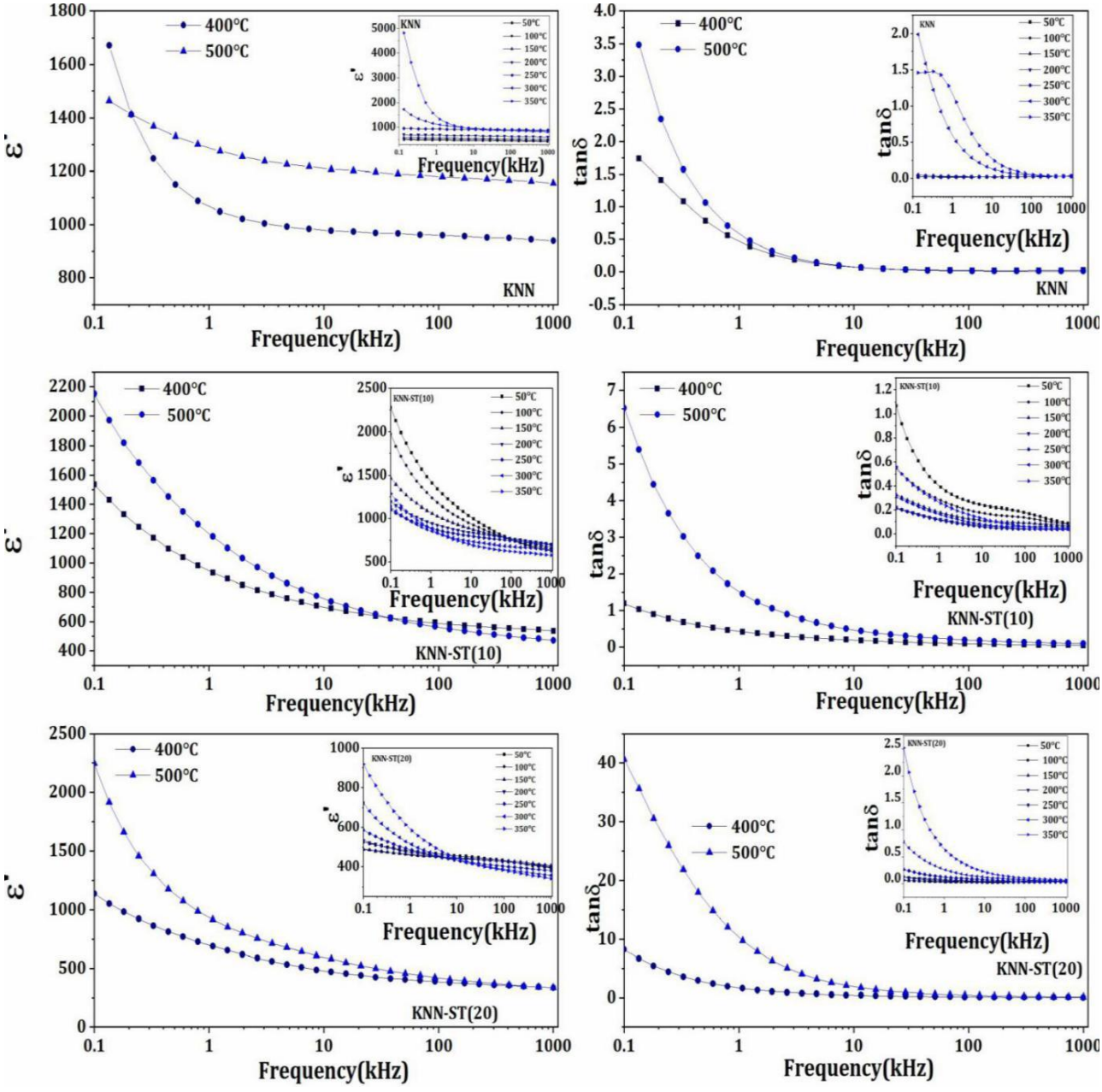


**Figure 4.7: Frequency dependent dielectric graph of (1-x)KNN(x)ST Solution for (x=0, 0.1, 0.2) at temperature range from room temperature to 500˚C.**

## 4.6 Impedance studies

Figure 4.8 represents the real part of impedance **(Z′)** as a function of frequency at temperatures ranging from 50˚C to 500˚C for (1-x) KNN-(x) ST ceramics (x=0,0.1, 0.2). Figure 4.8(a) clearly show higher values at low frequencies and is found to decrease at higher frequencies for undoped KNN. Figure 4.8(b) & (c) shows **Z′**of KNN-ST(10) and KNN-ST(20) ceramics as a function of frequency at different temperatures. **Z′** decreased at high frequencies and at high temperatures like KNN ceramics but at low frequencies and low temperatures, KNN-ST(10) and KNN-ST(20) ceramics exhibits higher **Z′** values than undoped KNN. This anomalous behaviour of impedance spectroscopy of (1-x) KNN-(x) ST could be attributed to small grain size of KNN-ST ceramics [37].

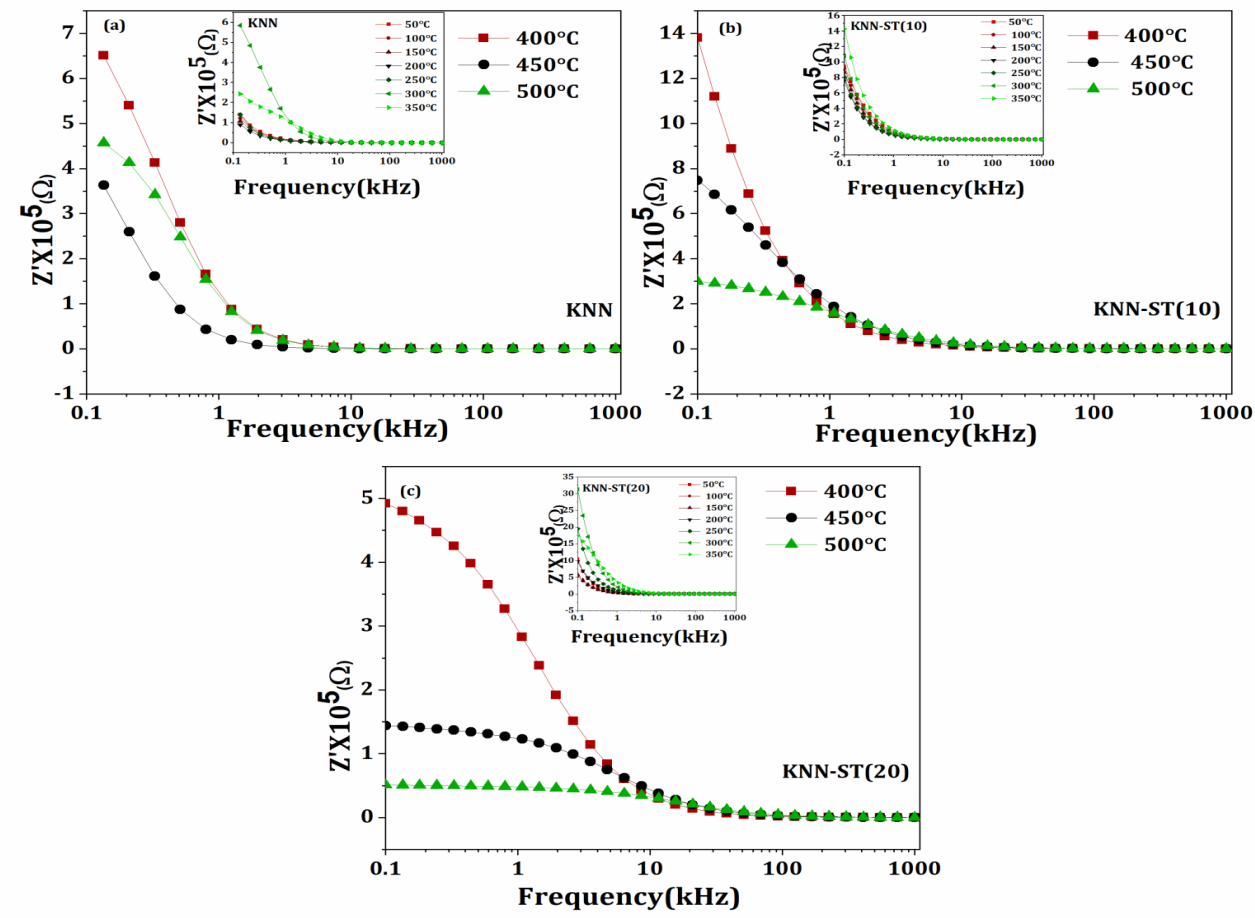


**Figure 4.8: Impedance (real part) graphs of (1-x)KNN-(x)ST solution at high temperature range and under inset Impedance(real part) graphs of (1-x)KNN-(x)ST solution at low temperature range are shown.**

Figure 4.9 represents the imaginary part of impedance (Z") as a function of frequency in temperature range 50˚C to 500˚C for (1-x) KNN-(x) ST solution (x=0, 0.1, 0.2). Figure 4.9(a)

shows that Z"of undoped KNN first increases with increase in frequency and temperature and reached at maximum value and from this point impedance value starts decreasing. Figure 4.9(b) & (c) show similar trends for KNN-ST(10) and KNN-ST(20) ceramics. KNN-ST ceramics show much higher value of imaginary part of impedance as compared to KNN. This behaviour of impedance indicates that (1-x) KNN-(x) ST shows dielectric relaxation behavior. *Guo et al., 2004* reported with addition $SrTiO_3$ into KNN ceramics[37].

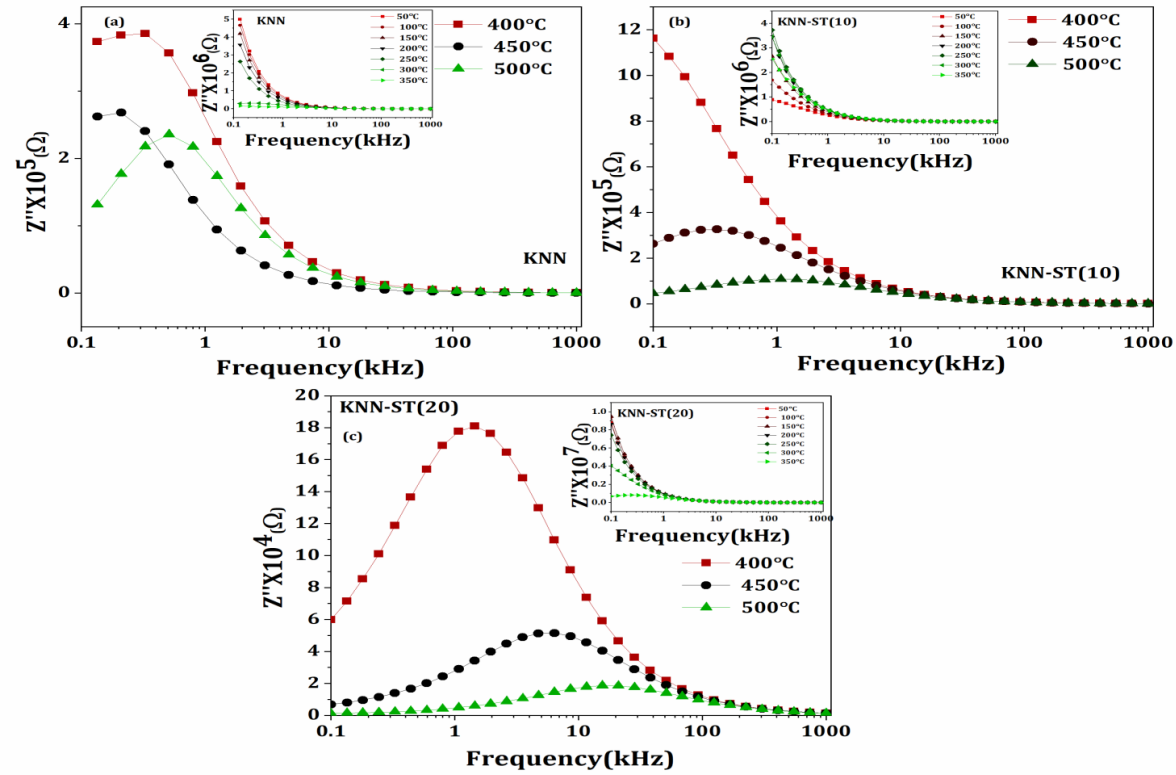


**Figure 4.9: Impedance (imaginary part) graphs of (1-x)KNN-(x)ST solution at high temperature range and under inset Impedance(imaginary part) graphs of (1-x)KNN-(x)ST solution at low temperature range are shown.**

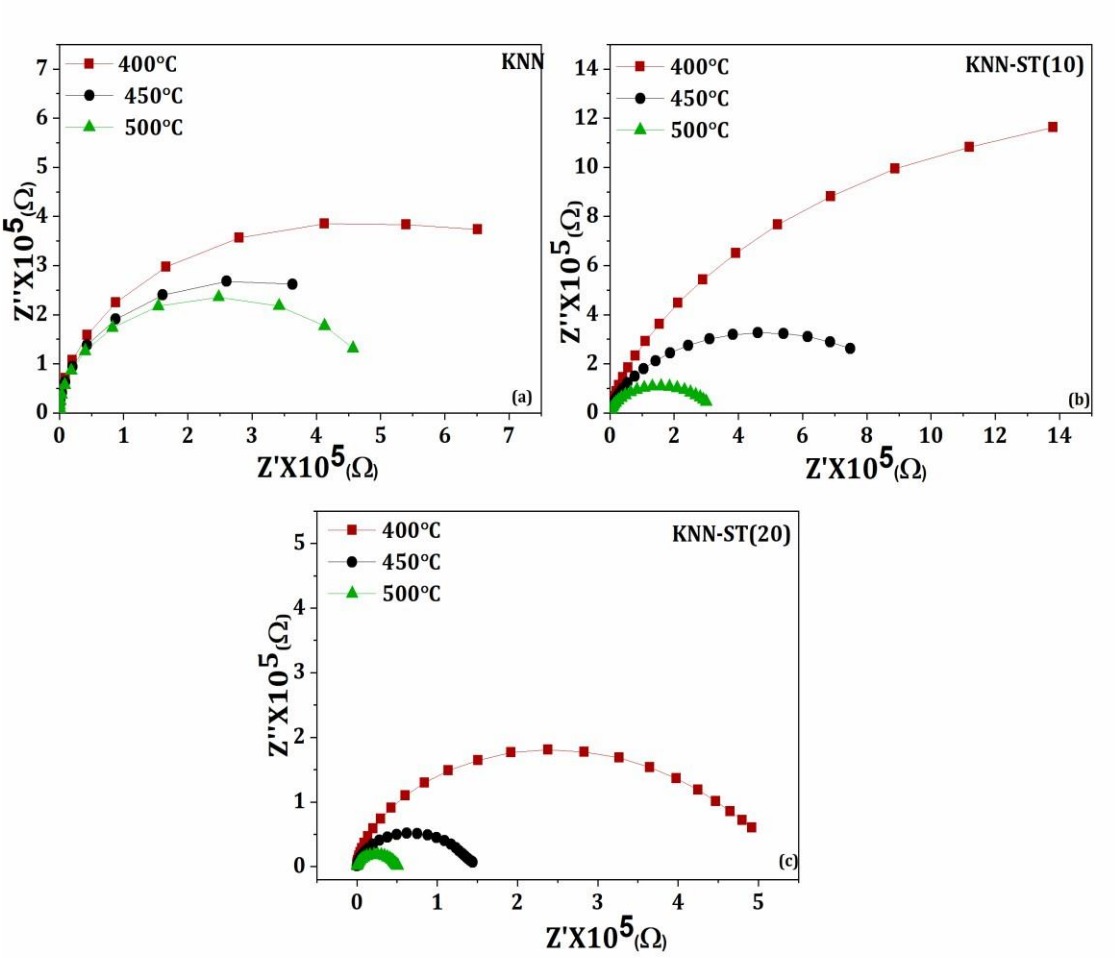


**Figure 4.10: Nyquist plots of (1-x) KNN-(x)ST solution at high temperature range.**

Figure 4.10 exhibits the Nyquist plots of (1-x) KNN- (x) ST ceramics (i.e. x=0, 0.1, 0.2) at high temperatures. Semicircular arcs are observed with addition of $SrTiO_3$ doped samples at different temperatures. In case of KNN proper semi circles are not observed at low impedance values but these semicircles are completes at high impedance values according to reported literature. This Nyquist plots indicate that (1-x) KNN-(x) ST is good insulating material. A decrease in bulk resistance is observed with increase in $SrTiO_3$. [38].

## 4.7. Optical studies

Optical study of undoped KNN and $SrTiO_3$ doped ceramics are represented by Figure 4.11 and 4.12. Figure4.11(a), (b) & (c) shows optical absorbance(%) with wavelength ranging from 200nm to 1000nm of (1-x)KNN-(x)ST solution for (x=0, 0.1, 0.2).

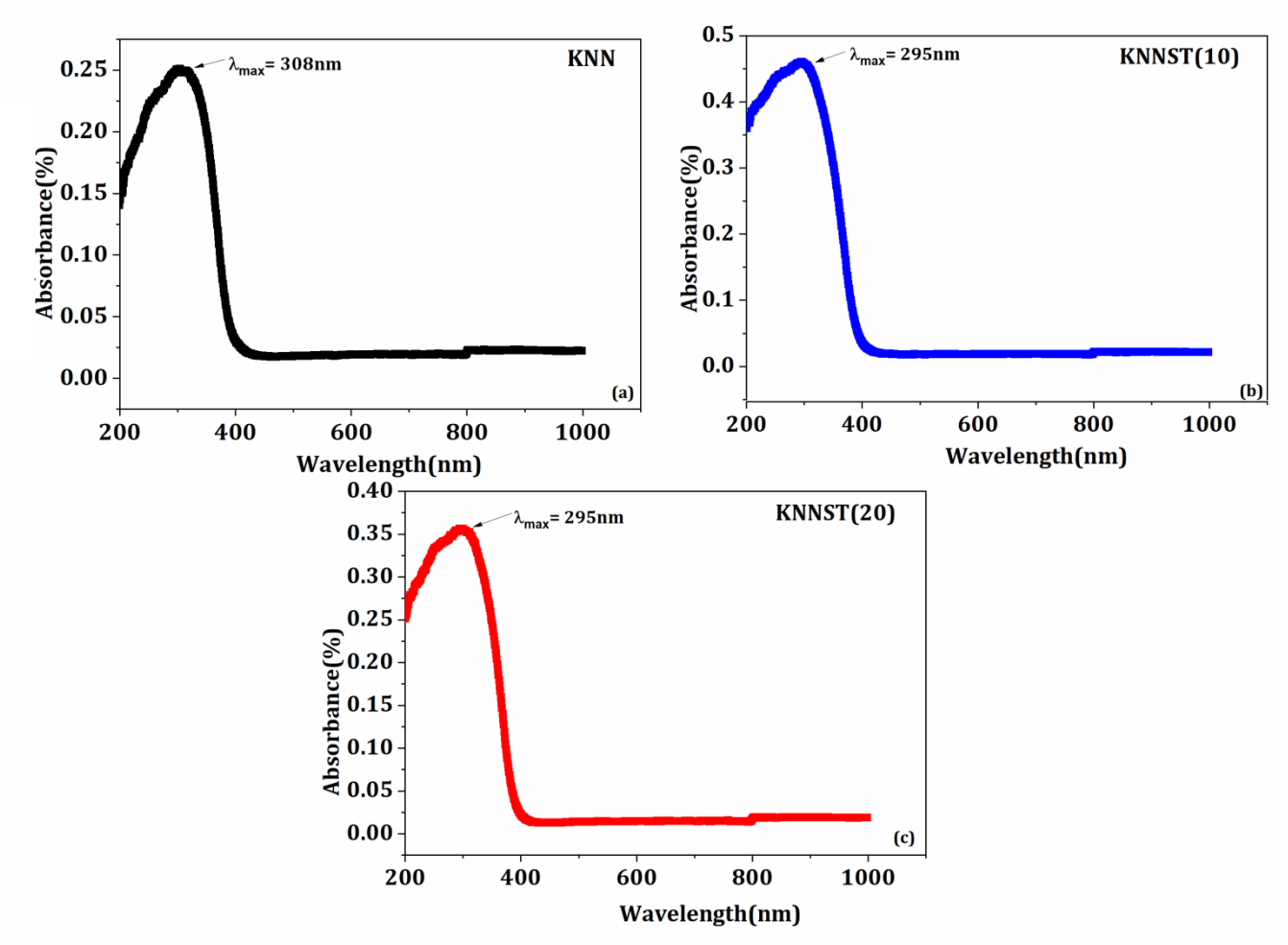


**Figure 4.11: Optical absorbance Vs.Wavelength study of (a) undoped KNN (b)KNN-ST(10) (c) KNN-ST(20)**

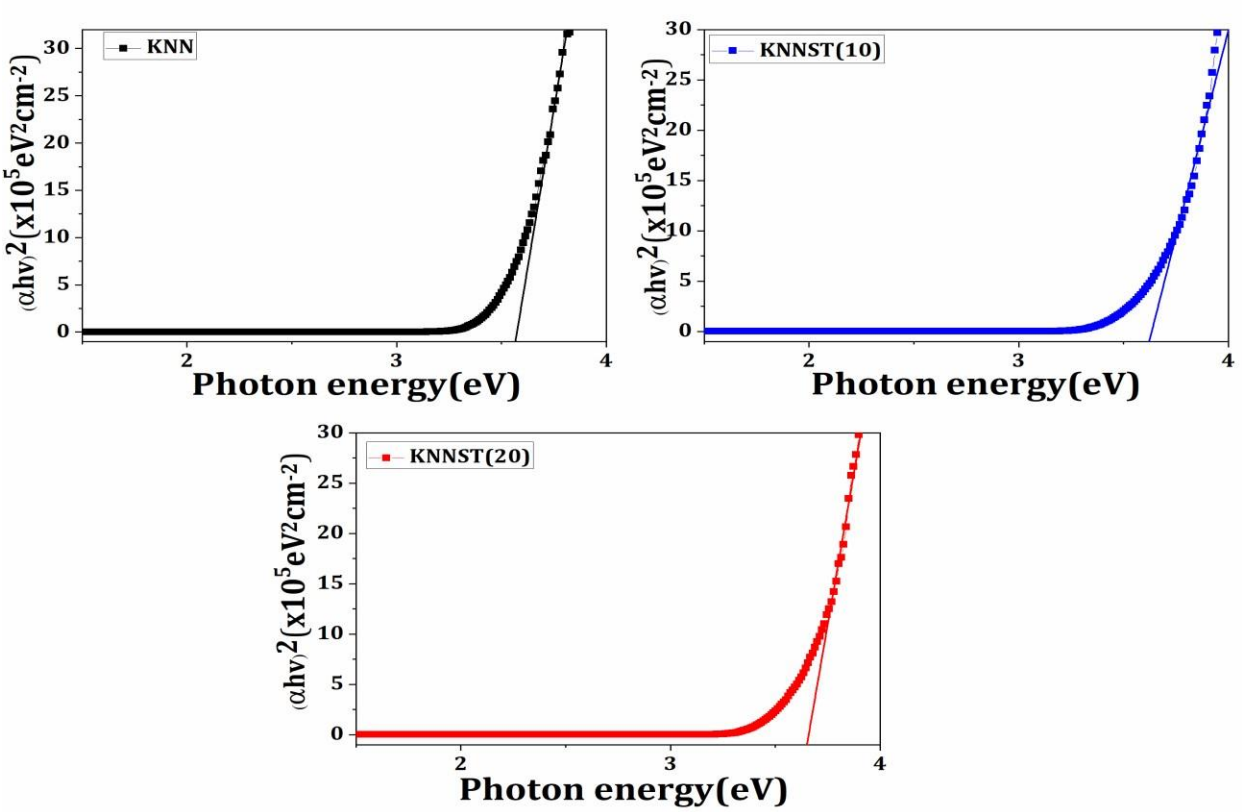


**Figure 4.12: Tauc plots of (1-x)KNN-(x)ST solution for composition x=0, 0.1, 0.2.**

Figure 4.12 shows Tauc's plots for $(1-x)K_{0.5}Na_{0.5}NbO_3$-$(x)SrTiO_3$ ceramics for all composition (x=0, 0.1, 0.2). Tauc's plots calculate the optical band gap energy ($E_g$). The band gap of KNN, KNNST(10),KNNST(20) ceramics are 3.57eV, 3.62eV, 3.65eV. Hence band gap is found to increase with the addition of $SrTiO_3$ into KNN ceramics[39].

## Conclusion

A detailed and systematic study of (K, Na)$NbO_3$-$SrTiO_3$ ceramics were carried out and the main highlights of the work are summarized as follows:

XRD pattern of (1-x)(K, Na)$NbO_3$-(x)$SrTiO_3$ solution exhibited a single phase of crystal structure, coexistence of orthorhombic -tetragonal symmetry is observed for (K, Na)$NbO_3$-$SrTiO_3$ ceramics which is evident from merging of the splitted peaks of undoped KNN into single peak Microstructural studies of these samples revealed that with addition of $SrTiO_3$ material into (K,Na)$NbO_3$, the grain size of (K, Na)$NbO_3$-$SrTiO_3$ ceramics decreased but porosity increased.

Dielectric studies of these samples confirmed that undoped KNN exhibits two dielectric peaks at 200˚C($T_d$) (orthogonal to tetragonal) and 430˚C($T_c$) (tetragonal to cubic), but with doping of $SrTiO_3$ into KNN, samples the dielectric peaks shifted to very low-temperature values. A typical relaxor behavior is observed for doped KNN ceramics. Impedance studies of undoped KNN and KNN-ST ceramics described that at low frequencies 100Hz, 1kHz impedance values increased and at high frequencies100kHz,1MHz impedance values decreased.

Ferroelectric hysteresis loop studies showed typical shaped ferroelectric hysteresis loop of undoped KNN which changed into a slim loop with doping of $SrTiO_3$ content and addition of $SrTiO_3$ energy storage density of ceramics increased and energy loss reduced.

Optical study explained that the energy band gap of KNN-ST is slightly greater than that of undoped KNN ceramics.

# Future Scope

The effect of sintering duration on the dielectric and ferroelectric properties of $(K,Na)NbO_3$ ceramics could be studied. $SrTiO_3$ doped $(K,Na)NbO_3$ ceramics exhibits low energy storage loss therefore these ceramics are good for investigation of energy storage study. High temperature ferroelectric measurements could be done to investigate electrocaloric applications.

## References

[1] Gao, J., Wang, Y., Liu, Y., Hu, X., Ke, X., Zhong, L., ... & Ren, X. (2017). Enhancing dielectric permittivity for energy-storage devices through tricritical phenomenon. *Scientific reports*, *7*, 40916.

[2] Benyoussef, M., Zannen, M., Belhadi, J., Manoun, B., Dellis, J. L., El Marssi, M., & Lahmar, A. (2018). Dielectric, ferroelectric, and energy storage properties in dysprosium doped sodium bismuth titanate ceramics. *Ceramics International*, *44*(16), 19451-19460

[3] Hao, J., Li, W., Zhai, J., & Chen, H. (2019). Progress in high-strain perovskite piezoelectric ceramics. *Materials Science and Engineering: R: Reports*, *135*, 1-57.

[4] Swain, S., Kumar, P., & Agrawal, D. K. (2013). Dielectric and ferroelectric study of KNN modified NBT ceramics synthesized by microwave processing technique. *Ceramics International*, *39*(3), 3205-3210.

[5] Chang, Y., Yang, Z., Wei, L., & Liu, B. (2006). Effects of AETiO3 additions on phase structure, microstructure and electrical properties of (K0. 5Na0. 5) NbO3 ceramics. *Materials Science and Engineering: A*, *437*(2), 301-305.

[6] Scott, J. F. (2007). Applications of modern ferroelectrics. *science*, *315*(5814), 954-959.

[7] http://research.physics.illinois.edu/Publications/theses/copies/fanning/3ferro.pdf

[8] Randall, C. A., Bhalla, A. S., Shrout, T. R., & Cross, L. E. (1990). Classification and consequences of complex lead perovskite ferroelectrics with regard to B-site cation order. *Journal of Materials Research*, *5*(4), 829-834.

[9] Xu, Y. (2013). *Ferroelectric materials and their applications*. Elsevier.

[10] Damjanovic, D. (1998). Ferroelectric, dielectric and piezoelectric properties of ferroelectric thin films and ceramics. *Reports on Progress in Physics*, *61*(9), 1267

[11] Wang, K., Yao, F. Z., Jo, W., Gobeljic, D., Shvartsman, V. V., Lupascu, D. C., ... & Rödel, J. (2013). Temperature-insensitive (K, Na) NbO3-based lead-free piezoactuator ceramics. *Advanced*

*Functional Materials*, *23*(33), 4079-4086.

[12] Kosec, M., Bobnar, V., Hrovat, M., Bernard, J., Malic, B., & Holc, J. (2004). New lead-free relaxors based on the K 0.5 Na 0.5 NbO 3–SrTiO 3 solid solution. *Journal of materials research*, *19*(6), 1849-1854.

[13] Barla, D. (2009). Synthesis of Tantalum Doped Sodium-Potassium Niobate System by Solid state Reaction Technique(Doctoral dissertation).

[14] Kozielski, L., Feliksik, K., Wodecka-Duś, B., Szalbot, D., & Tutu, S. (2018). Hot pressed $K_{0.5}Na_{0.5}nbo_3$ material for piezoelectric transformer for energy harvesting.

[15] Ishii, H., Nagata, H., & Takenaka, T. (2001). Morphotropic phase boundary and electrical properties of bisumuth sodium titanate–potassium niobate solid-solution ceramics. *Japanese Journal of Applied Physics*, *40*(9S), 5660.

[16] Lingwal, V., Semwal, B. S., & Panwar, N. S. (2003). Dielectric properties of Na 1-x K x NbO 3 in orthorhombic phase. *Bulletin of Materials Science*, *26*(6), 619-625.

[17] Guo, Y., Kakimoto, K. I., & Ohsato, H. (2005). (Na0. 5K0. 5) NbO3–LiTaO3 lead-free piezoelectric ceramics. *Materials Letters*, *59*(2-3), 241-244.

[18] Guo, Y., Kakimoto, K. I., & Ohsato, H. (2004). Ferroelectric-relaxor behavior of (Na0. 5K0. 5) NbO3-based ceramics. *Journal of Physics and Chemistry of Solids*, *65*(11), 1831-1835.

[19] Zuo, R., Fang, X., Ye, C., & Li, L. (2007). Phase Transitional Behavior and Piezoelectric Properties of Lead-Free (Na0. 5K0. 5) NbO3–(Bi0. 5K0. 5) TiO3 Ceramics. *Journal of the American Ceramic Society*, *90*(8), 2424-2428.

[20] Wang, R., Bando, H., Katsumata, T., Inaguma, Y., Taniguchi, H., & Itoh, M. (2009). Tuning the orthorhombic–rhombohedral phase transition temperature in sodium potassium niobate by incorporating barium zirconate. *physica status solidi (RRL)–Rapid Research Letters*, *3*(5), 142-144.

[21] López-Juárez, R., Novelo-Peralta, O., González-García, F., Rubio-Marcos, F., & Villafuerte-Castrejón, M. E. (2011). Ferroelectric domain structure of lead-free potassium-sodium niobate

ceramics. *Journal of the European Ceramic Society*, *31*(9), 1861-1864.

[22] Wang, X., Wu, J., Xiao, D., Zhu, J., Cheng, X., Zheng, T., ... & Wang, X. (2014). Giant piezoelectricity in potassium–sodium niobate lead-free ceramics. *Journal of the American chemical society*, *136*(7), 2905-2910.

[23] Wang, H., Zhao, X., Xu, J., Zhai, X., & Yang, L. (2016). Structure and properties of (1− x)[(K 0.5 Na 0.5) NbO3–LiSbO 3]–xBiFe 0.8 Co 0.2 O 3 lead-free piezoelectric ceramics. *Bulletin of Materials Science*, *39*(3), 743-747.

[24] Harttar, M. A. M., RASHID, M. W. A., & Azlan, U. A. A. (2015). Physical and electrical properties enhancement of rare-earth doped-potassium sodium niobate (KNN): A review. *Ceramics–Silikáty*, *59*(2), 158-163.

[25] Koruza, J., Rožič, B., Cordoyiannis, G., Malič, B., & Kutnjak, Z. (2015). Large electrocaloric effect in lead-free K0. 5Na0. 5NbO3-SrTiO3 ceramics. *Applied Physics Letters*, *106*(20), 202905.

[26] Liu, Z., Fan, H., Lei, S., Wang, J., & Tian, H. (2016). Fatigue properties and impedance analysis of potassium sodium niobate–strontium titanate transparent ceramics. *Applied Physics A*, *122*(10), 900.

[27] Yang, Z., Zhang, X., Yang, D., Yang, B., Chao, X., Wei, L., & Yang, Z. (2016). Excellent transmittance induced phase transition and grain size modulation in lead-free (1–x)(K0. 5Na0. 5) NbO3–xLaBiO3 ceramics. *Journal of the American Ceramic Society*, *99*(6), 2055-2062.

[28] Su, H. H., Hong, C. S., Tsai, C. C., Chu, S. Y., & Lin, C. S. (2016). Effect of microstructure on the dielectric properties of (1− x) Na0. 5K0. 5NbO3–xSrTiO3 ceramics. *Ceramics International*, *42*(15), 17558-17564.

[29] Gupta, A., Kumar, R., & Singh, S. (2018). Coexistence of negative and positive electrocaloric effect in lead-free 0.9 (K0. 5Na0. 5) NbO3-0.1 SrTiO3 nanocrystalline ceramics. *Scripta Materialia*, *143*, 5-9.

[30] Kumar, R., & Singh, S. (2018). Giant electrocaloric and energy storage performance of [(K 0.5

Na 0.5) NbO 3](1− x)-[LiSbO 3] x nanocrystalline ceramics. *Scientific reports*, *8*(1), 3186.

[31] Wegrzyn, M. (2012). *Sodium potassium niobate based piezoelectric ceramics* (Doctoral dissertation, The University of Manchester (United Kingdom)).

[32] Bhowmick, T. (2011). *characterizations of BNT ceramics synthesized by different techniques* (Doctoral dissertation).

[33] Yang, Z., Du, H., Qu, S., Hou, Y., Ma, H., Wang, J., ... & Xu, Z. (2016). Significantly enhanced recoverable energy storage density in potassium–sodium niobate-based lead free ceramics. *Journal of Materials Chemistry A*, *4*(36), 13778-13785.

[34] Su, H. H., Hong, C. S., Tsai, C. C., Chu, S. Y., & Lin, C. S. (2016). Effect of microstructure on the dielectric properties of (1− x) Na0. 5K0. 5NbO3–xSrTiO3 ceramics. *Ceramics International*, *42*(15), 17558-17564.

[35] Yang, Z., Du, H., Qu, S., Hou, Y., Ma, H., Wang, J., ... & Xu, Z. (2016). Significantly enhanced recoverable energy storage density in potassium–sodium niobate-based lead free ceramics. *Journal of Materials Chemistry A*, *4*(36), 13778-13785.

[36] Fan, H. Q., Li, Z., Ren, P. R., & Jiao, G. C. (2010). Relaxor Ferroelectricity and Electrostrictive Behavior of KNN-ST Ceramics. In *Materials Science Forum* (Vol. 654, pp. 1978-1981). Trans Tech Publications.

[37] Palei, P., & Kumar, P. (2011). Impedance spectroscopy and AC conductivity studies of ferroelectric (K0. 5Na0. 5) NbO3 ceramics. *Journal of advanced dielectrics*, *1*(03), 351-356.

[38] Echeverri, E., & Arnache, O. (2016, February). Structural and impedance analysis of Co-doped SrTiO3 perovskite. In *Journal of Physics: Conference Series* (Vol. 687, No. 1, p. 012040). IOP Publishing.

[39] Liu, Z., Fan, H., Zhao, Y., & Dong, G. (2016). Optical and tunable dielectric properties of K0. 5Na0. 5NbO3–SrTiO3 ceramics. *Journal of the American Ceramic Society*, *99*(1), 146-151.